International Journal of
Molecular Sciences

MDPI

Review

Complex Interplay of Heme-Copper Oxidases with Nitrite and Nitric Oxide

Jinghua Chen, Peilu Xie, Yujia Huang and Haichun Gao *

Institute of Microbiology, College of Life Sciences, Zhejiang University, Hangzhou 310058, China; cjh188@zju.edu.cn (J.C.); 21907023@zju.edu.cn (P.X.); 3180102131@zju.edu.cn (Y.H.)
* Correspondence: haichung@zju.edu.cn

Abstract: Nitrite and nitric oxide (NO), two active and critical nitrogen oxides linking nitrate to dinitrogen gas in the broad nitrogen biogeochemical cycle, are capable of interacting with redox-sensitive proteins. The interactions of both with heme-copper oxidases (HCOs) serve as the foundation not only for the enzymatic interconversion of nitrogen oxides but also for the inhibitory activity. From extensive studies, we now know that NO interacts with HCOs in a rapid and reversible manner, either competing with oxygen or not. During interconversion, a partially reduced heme/copper center reduces the nitrite ion, producing NO with the heme serving as the reductant and the cupric ion providing a Lewis acid interaction with nitrite. The interaction may lead to the formation of either a relatively stable nitrosyl-derivative of the enzyme reduced or a more labile nitrite-derivative of the enzyme oxidized through two different pathways, resulting in enzyme inhibition. Although nitrite and NO show similar biochemical properties, a growing body of evidence suggests that they are largely treated as distinct molecules by bacterial cells. NO seemingly interacts with all hemoproteins indiscriminately, whereas nitrite shows high specificity to HCOs. Moreover, as biologically active molecules and signal molecules, nitrite and NO directly affect the activity of different enzymes and are perceived by completely different sensing systems, respectively, through which they are linked to different biological processes. Further attempts to reconcile this apparent contradiction could open up possible avenues for the application of these nitrogen oxides in a variety of fields, the pharmaceutical industry in particular.

Keywords: nitrite; nitric oxide; heme-copper oxidase; proton-pumping

Citation: Chen, J.; Xie, P.; Huang, Y.; Gao, H. Complex Interplay of Heme-Copper Oxidases with Nitrite and Nitric Oxide. *Int. J. Mol. Sci.* **2022**, *23*, 979. https://doi.org/10.3390/ijms23020979

Academic Editor: Sergey Siletsky

Received: 21 December 2021
Accepted: 15 January 2022
Published: 17 January 2022

1. Introduction

Proton motive force (pmf) is essential for bacteria to grow and survive under non-replicating conditions by providing energy for a wide range of crucial processes [1–3]. The pmf (electrochemical potential) consists of two gradients: the chemical proton or pH gradient (ΔpH) and the membrane potential generated by the transport of electrical charge (Δψ). Bacteria are capable of generating the pmf by a variety of mechanisms; among them, the most efficient one is through oxygen reduction [3]. The oxygen-reducing enzymes (terminal oxidases) that contribute to the pmf generation are classified into two main groups: heme-copper oxidase (HCO) (also called heme-copper oxygen reductase (HCOR)) superfamily and *bd*-type quinol oxidase (*bd* QO) family [4,5].

The HCO superfamily is composed of three subfamilies, A, B, and C, as well as the structurally-related nitric oxide (NO) reductases (NOR) [6,7]. A-family HCOs include cytochrome *c* oxidases (C*c*Os), such as aa_3 from eukaryotic mitochondria, and some prokaryotes (often as caa_3, where *c* represents a cytochrome *c* subunit), and QOs, such as bo_3 of *Escherichia coli* [8–10]. HCOs of B and C families are present only in prokaryotes, with ba_3 and cbb_3 as respective representatives [9,11]. HCOs are highly efficient and specialized in pmf generation during the exothermic four-electron reduction of O_2 because of the proton-pumping mechanism [12,13]. In contrast, *bd* QOs, found exclusively in prokaryotes

to date, do not pump protons and are thus less efficient in energy conservation, but play an important role in mediating viability under various stress conditions [14,15].

Although HCOs of A, B, and C families are diverse in terms of subunit composition, electron donor, and heme type, they house a similar signature active site, the so-called binuclear center (BNC), where the reduction chemistry occurs [7]. Located in a subunit with 12 membrane-spanning helices, this BNC consists of two magnetically coupled redox-active metal centers, a high-spin heme (a_3, o_3, or b_3), and a copper ion (Cu_B) [7,8,11,16]. In all HCOs, these two metal centers are in proximity, with the two metals (Fe and Cu) only ~5 Å apart [7,17]. During the oxygen reduction, the BNC experiences an oxidative-to-reductive phase transition involving several intermediate states [18].

Nitrogen is essential to all life and is a constituent element of amino acids, proteins, and nucleic acids. After fixation, nitrogen as nitrogen gas (N_2), the most abundant element in the atmosphere, can be converted to ammonium and a variety of nitrogen oxides, among which nitrite (NO_2^-) and nitric oxide (NO) are the most common and bioactive species [19,20] (Figure 1). Given that bacteria are able to catalyze all steps of the nitrogen cycle, they are crucial for the inter-conversion of different nitrogen oxides [21]. Both nitrite and NO are involved in diverse physiological processes in bacteria functioning as important cellular signaling molecules, substrates of metabolic enzymes, and inhibitory agents modulating protein activity [19,22]. Although a significant portion of phenotypic changes caused by nitrite are NO-independent, it is widely accepted that NO is the molecule largely underpinning the physiological influences; nitrite impacts the physiology of living organisms in part by serving as a biochemical circulating reservoir for NO [19]. Additionally, NO can be engaged in cellular physiological and pathological processes through a complex cross-talking with two other gasotransmitters, carbon monoxide (CO) and hydrogen sulfide (H_2S) [23–27]. Meanwhile, nitrite can be converted back to NO through the one-electron-oxidation of NO.

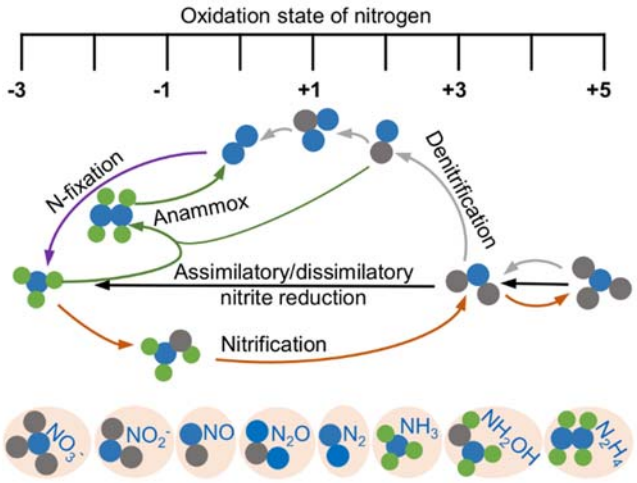

Figure 1. Redox cycle for nitrogen driven by prokaryotes. Shown are the major biological nitrogen transformation pathways, each of which are represented by lines in the same color, and the relative oxidation state at which they occur.

Given the particular importance of the inter-conversion of nitrite and NO, bacteria have evolved a variety of enzymes to catalyze the transformation of nitrite and NO, including NOR [19,28]. In addition, although the HCOs of all A, B, and C families differ from NOR in their metal ions within the BNCs, they are also profoundly implicated in the biology of nitrogen oxides. The direct reactions of HCOs with nitrite and NO, which have been known for a long time, provide a mechanistic understanding of the interplay between the enzymes and the two nitrogen oxides [29,30]. On one hand, it is well known that eukaryotic C*c*Os mediate the reduction of nitrite to NO under hypoxic conditions [31,32]. On the other hand, bacterial HCOs (ba_3, caa_3, bo_3) of the A and B families are capable of catalyzing the reduction

of NO to N_2O, whereas C-family HCOs (cbb_3) convert nitrite to N_2O [19,33–35]. On the other hand, both nitrite and NO are bacteriostatic agents due to their ability to inhibit proteins, especially hemoproteins [36,37]. A great body of evidence has been accumulated showing that nitrite and NO react with purified HCOs and *bd* QOs in vitro and inhibit cell respiration in vivo [22,30,31,38–42]. While there are common reaction mechanisms involved in the inhibition by nitrite and NO, considerable discrepancies have been observed between their cellular targets identified to date [22]. Thus, the extent of the effective mechanisms elucidated by in vitro analyses is in living cells is still a matter of study.

In this review, we aim to present recent findings in the context of the current understanding of the interactions of HCOs with nitrite and NO. It begins with a concise introduction of structural and functional properties of HCOs and *bd* QOs, which serves as the basis for comprehension of the mechanistic characteristics of the interaction. By comparing nitrite and NO, in terms of their biochemical features and physiological impacts in bacteria, we evaluate the presently accepted "avenues" of nitrite and NO and the discrepancy between in vitro and in vivo analyses. The knowledge summarized here encourages future investigations into new potential pathways, new functions, and new mechanisms regarding how living organisms exploit nitrite and NO while preventing their damages.

2. Bacterial Terminal Oxidases for pmf Generation

Proton translocation across the membrane is of crucial importance for sustaining the cellular activity in all organisms. However, due to the polarity characteristics, protons are unable to pass through the phospholipid-bilayer membrane freely by diffusion like small non-polar molecules. Proton pumps are special and efficient hydrogen ion transporters that move protons across the membrane from the low-concentration side to the high-concentration side to form pmf, which is subsequently utilized to drive the production of adenosine triphosphate (ATP), the cell's chemical energy currency, by ATP synthase [1–3].

In aerobic bacteria, transmembrane proton pumping is closely related to the oxidative phosphorylation process, especially with the terminal oxidases in the respiratory chain. The bacterial terminal oxidases, including HCOs of the A, B, and C families and *bd* QOs, catalyze the four-electron reduction of oxygen to water using quinol or cytochrome *c* as the electron donors. The main role of most HCOs in microbial metabolism is to conserve energy [43–45], and *bd* QOs are thought to contribute to nitrosative stress tolerance, hydrogen peroxide detoxification, or prevention of H_2S toxicity, especially in pathogenic bacteria [42,46–49]. To date, a number of high-resolution structures of terminal oxidases from each group have been reported, which have greatly enhanced our understanding of the exact working mechanism of these enzymes.

2.1. HCOs

HCOs are the most extensively studied terminal oxidases. Despite the variety in the composition of the electron donor, polypeptide, and heme group type, all HCOs possess a conserved redox center composed of a low-spin heme and a heteronuclear heme-copper center (binuclear center, BNC) consisting of a high-spin heme and a copper (Cu_B) [44,50]. Based on the amino acid sequences and the proton-pumping pathways, members of the HCO superfamily are divided into three families as A, B, and C [51] (Figure 2A).

Bacterial A-family HCOs include aa_3-type C*c*Os (aa_3-HCO, in some cases caa_3-HCO), which exhibit high structural relations to their mitochondrial counterparts, which contain only *a*-type hemes, and the bo_3-type QOs (bo_3-HCO) from *E. coli* (Figure 2A). Most often, A-family HCOs contain three subunits, named SU-I, II, and III. SU-I is highly conserved among all HCOs and typically composed of 12 transmembrane helices (TMHs), which hold the BNC [43]. SU-II contains a membrane-anchored cupredoxin domain functioning for harboring the mixed-valence di-nuclear copper (Cu_A) acting as the primary electron acceptor [43]. The divalent cations (Mg^{2+} or Mn^{2+}) located at the interface between SU-I and SU-II and close to the high spin heme in HCOs of A and C families are not essential for proton pumping; however, their exact functions remain unclear [52,53]. SU-III is present

in most bacterial A-family HCOs and possibly influences the oxygen reduction as well as the internal proton flow [43]. An additional subunit (SU-IV) is also identified in A-family HCOs, with its function a mystery yet [10,11,16].

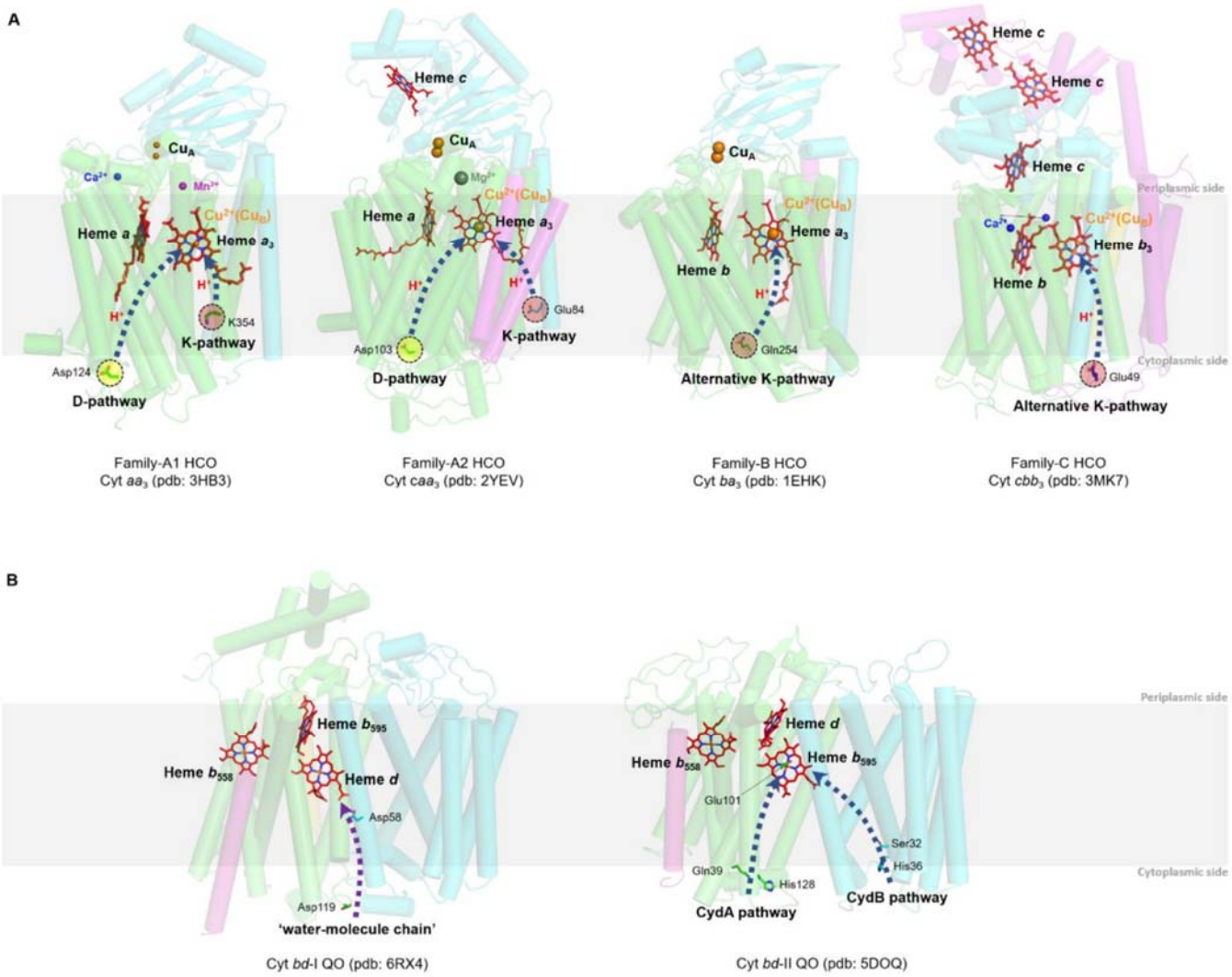

Figure 2. Prosthetic group arrangements and proton pathways of typical bacterial HCOs (**A**) and bd QOs (**B**). (**A**) Representative structures of HCOs of A (divided into A1 and A2), B, and C subfamilies. Protein peptides, heme cofactors, and ions are shown as cartoons, sticks, and spheres, respectively. SUs I of families A and B, SU III of family A and CcoN of family C are colored in green; SUs II of families A and B, and CcoO of family C are colored in cyan; SU IV of family A, SU IIa of family B, and CcoO of family C are colored in magenta; the 30-mer peptide in family C HCO is colored in yellow. The blue dashed arrows indicate the proton pathways inside each HCO, with the amino acid residues at the entry point of each pathway marked with dashed cycles. (**B**) Structures of Cyt bd-I and bd-II QOs. Protein peptides and heme cofactors are shown as cartoons and sticks with subunits CydA and CydB colored in green and cyan, and CydX in bd-I QOs and CydS in bd-II QOs colored in magenta, respectively. The purple dashed arrow indicates the 'water-molecule chain' observed between residues Asp119 (subunit A) and Asp58 (subunit B) in bd-I QOs. The blue dashed arrows indicate two proposed proton pathways in bd-II QOs. Figures are prepared with PyMOL (Molecular Graphics System, LLC) https://www.pymol.org (accessed on 20 December 2021).

B-family HCOs comprise similar subunit compositions but with low sequence homology to their A-family counterparts (Figure 2A). In contrast to the canonical composition of 12 TMHs in SU-I of A-family HCOs, SU-Is of B-family HCOs, as seen in C*c*Os from *Thermus thermophilus* and *Aquifex aeolicus*, possess 13 and 14 TMHs, respectively [54,55]. The SU-II

of B-family HCOs resembles its A-family counterpart in that both contain a membrane-anchored cupredoxin domain; however, an additional subunit (SU-IIa) consisting of a single helix is identified in the former [55]. The His-Tyr cross-link in A-family HCOs, which functions to fix Cu_B in a certain configuration and distance from heme a_3 at the BNC [56], is also conserved in B-family HCOs.

C-family HCOs are highly divergent from HCOs of the former two families in protein sequence (Figure 2A). To date, only *cbb*$_3$-type C*c*Os are reported in this group [11]. The SU-I of C-family HCOs contains a His-Tyr cross-link as well, but with the two residues residing at two separate helices different from the situations in HCOs of A and B families. In addition, C-family HCOs lack the di-nuclear copper site (Cu_A) but utilize two auxiliary heme-binding subunits (CcoO and CcoP) to receive electrons from reduced cytochromes [11]. C-family HCO contains an extra subunit CcoQ, a small non-heme protein that is not required for catalytic activity but has a role in the assembly of the HCO complex [57].

The proton pumping in A-family HCOs is performed via two pathways, D-pathway and K-pathway, named accordingly by the conserved and functionally critical residues (Aspartate and Lysine, respectively) near the entry site of each pathway (Figure 2A). In order to pump protons, A-family HCOs utilize the internal 'proton wires' to transfer the electronic charges in a way similar to the Grotthuss mechanism [3,58]. Within the longer D-pathway, a series of acid residues and water molecules jointly form a consecutive chain through hydrogen bonds and connect the entrance aspartate to the gating residue close to the BNC [59]. Due to the crucial role of the water molecules, a water gating proton pumping mechanism was thereby proposed in D-pathway [60]. A-family HCOs could be further divided into two types as A1 and A2, based on the residue composition at the hydrophobic end of the D-pathway. Type A1 is featured with a conserved glutamate within the motif XGHPEV on helix VI. However, in type A2, this residue is replaced by consecutive tyrosine and serine in a YSHPXV motif. HCOs of both types A1 and A2 have a covalent bond between one of the Cu_B-coordinated histidines and a tyrosine on the same helix [61]. The D-pathway is responsible for transporting six protons, four of which are pumped to the positive side (P-side) of the membrane; the remaining two are donated to the active site for use in oxygen reduction [43]. By contrast, the shorter K-pathway typically consists of a few highly conserved polar residues and only qualifies to supply two protons to the catalytic site during the initial reduction of the BNC [59]. A conserved binding domain (carboxyl group) for amphipathic compounds adjacent to the entrance of the K-pathway tends to play a role in organizing the water chain, which supports proton uptake [9,62,63].

The canonical K- and D- pathways are absent in either B-family or C-family HCOs; instead, an alternative K-pathway analogous to that in A-family HCOs is exploited [11,54] (Figure 2A). This K-pathway in B-family HCOs consist of a series of conserved polar residues that form a proton channel. Most of these residues reside within SU-I, with an additional glutamate at the entry site on SU-II. C-family HCOs possess an alternative K-pathway structurally similar to that in B-family HCOs. Within the *cbb*$_3$-HCOs from *Pseudomonas stutzeri* and *Rhodobacter sphaeroides*, the proton pathway propagates through a few polar residues with the terminal residue tyrosine cross-linked to one of the histidine ligated to Cu_B [11,64].

All HCOs are electrogenic proton pumps, and the internal and intramolecular electron transfer pathways for each HCO family have been extensively studied [43,65–68]. The catalytic cycle of A-family HCOs includes two phases, an oxidative phase and a reductive phase, involving several intermediate states of the active site, fully oxidized (**O**, Fe^{3+} Cu_B^{2+}), single-electron reduced (**E**, Fe^{3+} Cu_B^{+} or Fe^{2+} Cu_B^{2+}), and two-electron reduced (**R**, Fe^{2+} Cu_B^{+}) (Figure 3) [18]. Upon O_2 binding to **R**, a short-lived new complex **A** is formed, which delivers electrons rapidly to bound O_2 for the cleavage of the dioxygen bond, forming intermediates **P** and **F** in sequence [69]. Both **P** and **F** are a ferryl derivative of (Fe^{4+} = O Cu_B^{2+}), but the former carries Y244 in the radical form, whereas the latter has Y244 reduced and protonated [31,70–72]. Eventually, the fully oxidized state **O** is regenerated from **F** after receiving an additional electron from CuA/heme *a*. During the oxygen reduction, the first

proton pumping event occurs during the **P** to **F** transition, and the reaction cycle completes when **R** is regenerated from **E** with two product water molecules released, and two protons pumped [73]. The source of the electron may be a tyrosine or tryptophan radical close to the active site; however, the exact identity of the amino acid, which provides this electron, is still under debate [43].

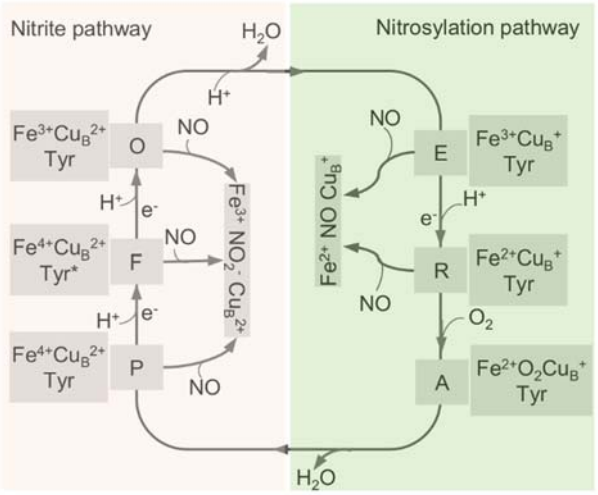

Figure 3. The catalytic cycle of HCO and the interplay with NO through the two pathways. The catalytic cycle of HCO is schematically reported with the indication of the redox and the oxygen ligation state of the BNC (heme a3-CuB active site). In the reductive phase, the oxidized species O is fully reduced to R by two single-electron donations via formation of the half-reduced intermediate E. In the oxidative phase, upon reaction with O_2, R converts to P and F, and O is regenerated eventually through further electron transfer. The nitrite-bound derivative (Fe^{3+} CuB^{2+} NO_2^-) and the nitrosylated adduct (Fe^{2+} CuB^+ NO) are generated by the reactions of these intermediates with NO. Tyr, CuB-interacting residue Y244, with an asterisk representing the radical form.

The proton-pumping loading sites in all HCOs are still controversial [74]. The histidines ligating the heme iron and Cu_B, as well as the A- and D- propionates of heme a_3 at the catalytic center have been proposed as candidate proton loading sites [75]. A hydrophilic cavity above the hemes, housing divalent cations or water molecules at the interspace of SU-I and SU-II, is possibly the beginning of the water exit pathway [10,11,16].

2.2. *bd* QO

bd QO is a quinone-type terminal respiratory enzyme that distributes widely in bacteria and archaea. Unlike HCOs that have two hemes and a copper in the active sites, *bd* QOs accept electrons from quinones (ubiquinol or menaquinol) to reduce oxygen to water using three hemes (Figure 2B) [14,76]. A few isoforms of the *bd* QO family contain only *b*-type hemes, which are less sensitive to inhibition by cyanide [77]. Initially, *bd* QO was considered to consist of two subunits only, named CydA and CydB, encoded by a single operon [78]. However, a small single-transmembrane subunit (CydX or CydS) encoded by the third gene in the *cyd* operon is found to be not only functionally essential but also involved in the assembly of the enzyme complex in some bacteria in recent years [79–81]. Based on the structural differences of the quinol binding sites (Q-loop), *bd* QOs are subdivided into L-subfamily (long Q-loop) and S-subfamily (short Q-loop) [14,82].

bd QO lacks a counterpart proton-pumping mechanism as in HCOs; instead, they generate a pmf through the transmembrane charge separation and the coupled Q-cycle [83]. There are two potential proton pathways, CydA and CydB pathways, through which protons could pass from the cytoplasm to the high-spin heme site (b_{595}) in *bd* QO from *Geobacillus thermodenitrificans* [15]. The proton transfer from heme b_{595} to the oxygen reduction site via heme *d* is possibly facilitated by water molecules or the heme propionates

of heme b_{595} [15]. To date, no oxygen channels have been found in *bd* QOs, implying that oxygen molecules likely approach heme *d* laterally from the alkyl chain interface with the membrane [15].

3. Roles of HCOs in the Transformation of Nitrogen Oxides

In addition to carrying out O_2 reduction, HCOs have been shown to be deeply implicated in the biotransformation of multiple nitrogen oxides. It is well recognized that mitochondrial aa_3-HCO is capable of reducing NO_2^- to NO under hypoxic conditions [20,35]. This reduction, which involves only one electron, differs from the four-electron reduction of O_2 to H_2O and is not involved with proton pumping [35]. Unlike their eukaryotic counterparts, bacterial HCOs, including the caa_3-HCO and ba_3-HCO from *T. thermophilus*, cbb_3-HCO from *P. stutzeri*, and bo_3-HCO from *E. coli*, are able to catalyze the reduction of NO to N_2O [36,84,85]. In addition, cbb_3-HCO of *P. stutzeri* is also able to reduce NO_2^- to N_2O directly [33].

Despite having been known for a long time, the interactions of nitrite with mitochondrial aa_3-HCO have not yet been addressed. Instead, the current understanding of the subject derives mainly from the reactions of nitrite with synthetic heme/copper assemblies [32,86,87] (Figure 4A). During catalytic turnover, the ferrous heme of the a_3-Cu_B BNC functions as the electron donor, while the Cu_B center serves as a Lewis acid for the cleavage of the N-O bond of nitrite [32]. The overall reaction is a one-electron reduction of nitrite, during which an oxygen atom derived from the nitrite is transferred to the BNC, resulting in an oxo-bridge Fe^{3+}-O-Cu^{2+} intermediate. Interestingly, this oxo-bridge Fe^{3+}-O-Cu^{2+} could also oxidize NO back to nitrite. It is speculated that the inter-conversion of nitrite and NO has important implications in the modulation of cellular O_2 balance [32,86,87]. When O_2 is limited, nitrite interacts with the BNC for reduction, generating NO. This NO molecule can reversibly inhibit the oxygen reduction at the same site, leading to O_2 accumulation. The reverse reaction is composed of the same steps traversed backward, and as a result, NO is converted back to nitrite for future use, and the enzyme is freed to catalyze the four-electron reduction of O_2 to water. The overall reaction is regarded as an adaptive mechanism alleviating NO-mediated respiratory inhibition [88].

Multiple lines of evidence suggest that eukaryotic and bacterial HCOs have different reactivities to nitrogen species [89]. In contrast to eukaryotic mitochondrial HCOs, the bacterial counterparts react with nitrite and NO, producing N_2O as the end product [33,34,89] (Figure 4B,C). Upon the addition of NO to oxidized ba_3-HCO (**O**) of *T. thermophilus*, a six-coordinate heme Fe^{2+}-NO species has been detected, suggesting that a hyponitrite ($HONNO^-$) ion bound to the BNC in the **E** state (Fe^{3+} Cu_B^+) is transiently formed [90]. Further investigations have demonstrated that the binding of two NO molecules to the BNC is accompanied by protonation of the heme a_3-NO species and the electron transfer from Cu_B^+, leading to the concomitant formation of the N-N bond. Eventually, N_2O and H_2O are released after additional H^+ is added and the N-O bond is cleaved. This mechanism has been observed in reactions of NO with caa_3-HCO, *bcc*-aa_3 supercomplex (formed by cytochrome *bcc* and aa_3-HCO in *Mycobacterium tuberculosis*), and bacterial NORs, suggesting a possibility that it is conserved in all enzymes of the HCO superfamily [91–94]. Despite this, the NO reductase activities of all HCOs tested so far are substantially lower than those observed with bacterial NORs, implying that their contribution to NO reduction is likely to be limited unless NORs are absent [85,95]. In addition, the ba_3-HCO of *T. thermophilus* also interacts with nitrite to form a ferrous heme a_3-nitro complex in the BNC, but NO or N_2O is not produced above the detection limit, suggesting that this enzyme is likely to be susceptible to nitrite inhibition, as discussed below [89].

On the contrary, under reducing conditions, nitrite reacts with cbb_3-HCO to form a six-coordinate ferrous heme b_3-nitrosyl complex [33]. The binding of NO_2^- to heme b_3 triggers electron transfer from the heme to the substrate, leading to its double protonation reduction to NO and release of a H_2O molecule. Heme b_3 is concomitantly re-reduced with electrons from either Cu_B or heme *b*, which is turned toward heme b_3 for creating van

der Waals contacts between the hemes [11]. As a result, the ferrous six-coordinate heme b_3–nitrosyl complex is formed, which has NO-trapping activity such that the subsequent catalytic reduction to N_2O could occur [33]. As the van der Waals contact is missing in other HCO families, it may explain why the reduction of NO_2^- to N_2O is only observed with cbb_3-HCO [11]. Moreover, given that the reduction of NO by cbb_3-HCO involves a five-coordinate ferrous heme b_3–nitrosyl adduct [56], five- and six-coordinate heme b_3–nitrosyls likely exist in equilibrium in the reduction, and their ratio may vary depending on experimental conditions [33].

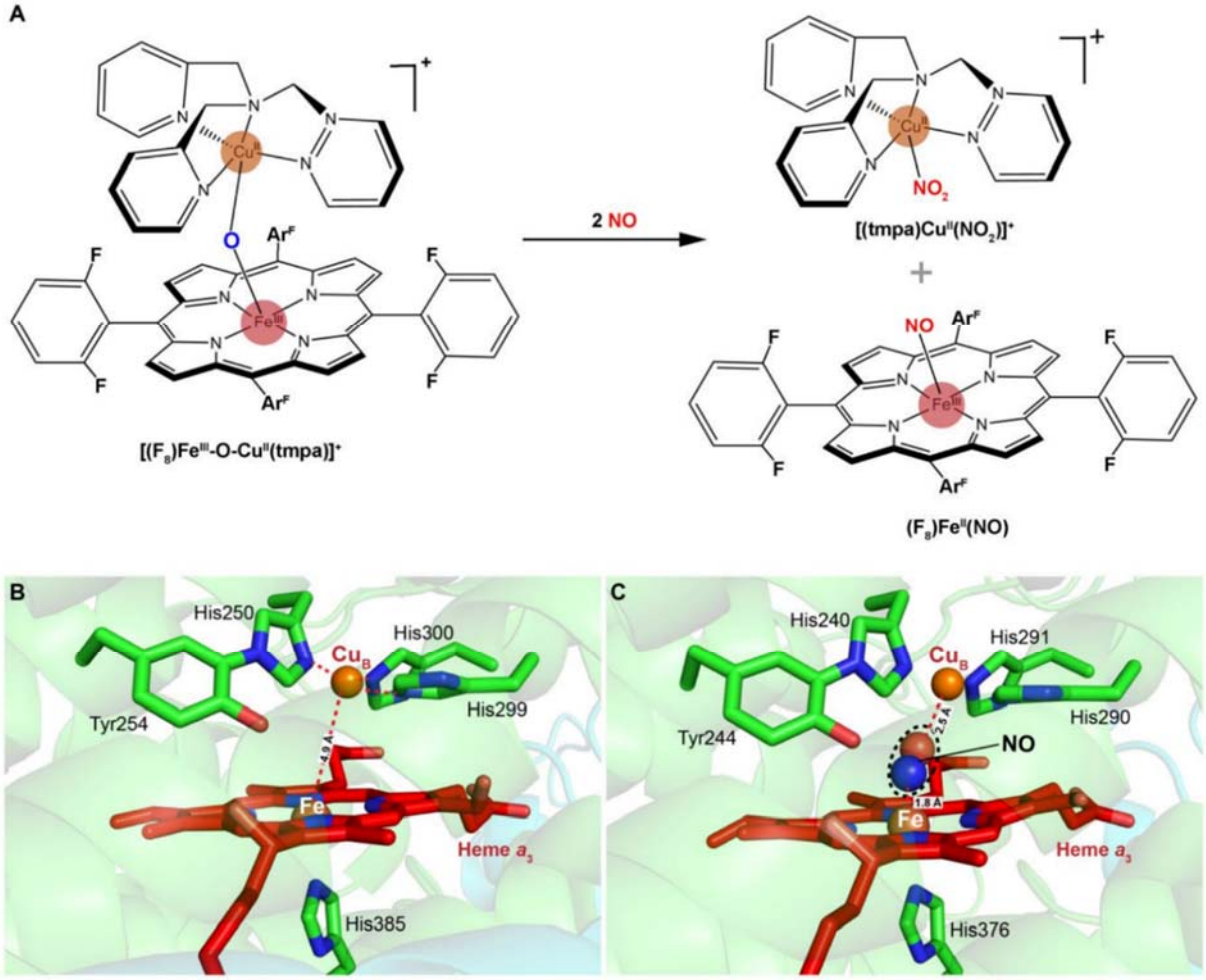

Figure 4. Scheme of a heme-copper assembly mediated oxidation of NO to nitrite and structures of ligand-absent and NO-binding BNCs of CcOs. (**A**) A μ-oxo heme-FeIII-O-CuII complex facilitates NO oxidation to nitrite, forming reduced heme and CuII-nitrito complexes. This scheme is modified from the figure in reference [26] with ChemDraw. (**B**) Spatial structure of the BNC of Cyt caa3 oxidase from *T. thermophilus* HB8. The copper atom (CuB) is coordinated by three histidine residues. The distance between CuB and heme-iron is less than 5 Å. (**C**) X-ray structure of the NO-bound CcO from bovine CcO. The distances between CuB and oxygen atom from NO, heme-Fe, and nitrogen atom from NO are 2.5 Å and 1.8 Å, respectively. Figures of B and C are prepared with PyMOL (Molecular Graphics System, LLC) https://www.pymol.org (accessed on 20 December 2021).

4. Inhibition of HCOs by Nitrite and NO

To date, a large number of HCO inhibitors have been known, and the repertoire is still expanding [96,97]. These HCO inhibitors interact with the BNC directly and thus are substantially less effective on other terminal oxidases that do not pump protons. In general, HCO inhibitors can be divided into four categories: (i) heme-binding inhibitors competitive with oxygen (CO and NO, etc.); (ii) heme-binding inhibitors not competitive

with oxygen (cyanide (CN^-), H_2S, and azide (N_3^-), etc.); (iii) inhibitors which act by preventing binding of cytochrome *c* to C*c*O (alkaline proteins and polypeptides, etc.); (iv) Quinol-like compounds acting at the Q binding site of QOs [97].

Inhibition of the BNC by CN^-, H_2S, and N_3^- has been intensively investigated, offering the best illustration of the mechanisms underpinning the oxygen-binding and proton pumping [98,99]. Three forms of mitochondrial aa_3-HCOs in the **O** state have been defined by the difference in the cyanide binding rates, namely, "slow", "fast", and "open" forms [100,101]. During the catalytic turnover, the open form resulting from O_2 oxidation of the **R** state has Fe^{3+}-OH^- as the iron coordination structure of the O_2 reduction site, allowing proton pumping after each of the first and second single-electron donations to the fully oxidized enzyme [102]. The nature of the ligands that bind to the BNC is still uncertain, and the proposed include a peroxide group bridging the two metal sites in the O_2 reduction site (Fe^{3+}-O-O-Cu^{2+}), superoxide, hydroxide, water, and even oxygen [103–105]. Most recently, it has been suggested that a radical Tyr-288 is present in the fast form and a protonated Tyr-288 in the slow form [106]. Nonetheless, in contrast to the open form, neither the fast form nor the slow form induces proton pumping [102]. As the rate of CN^- binding to the open form is substantially higher than the binding rate to the other two forms; the proton-pumping is highly sensitive to cyanide [107].

The reactions between mitochondrial aa_3-HCO and NO were first described more than four decades ago [29]. The NO inhibition of aa_3-HCO is rapid and reversible and may occur in competition with oxygen. Inhibition takes place following two different pathways, the nitrosylation pathway and the 'nitrite' pathway [30] (Figure 3). In the nitrosylation pathway, a relatively stable (Fe^{2+} NO Cu_B^+) nitrosyl-derivative of the **R** state is formed when **E** or **R** reacts with NO [31,71,88,108]. Given that the stable nitrosyl adduct can be formed at a rate comparable to that of O_2, it is apparent that the reduction of the BNC and its stabilization in the nitrosylated state are equally favored [109]. One of the peculiar properties of the stable nitrosyl adduct is that it would not modify NO, and as a result, NO can be released unaltered [31]. This likely explains why mitochondrial aa_3-HCO loses the ability to reduce NO to N_2O because NO can be released [110]. In addition, the rate of NO dissociation from reduced aa_3-HCO is unusually high, at least an order higher than that of other hemoproteins such as hemoglobin [111]. A consequence is that the activity can be rapidly recovered after NO is removed, although aa_3-HCO is promptly inhibited upon NO exposure.

Alternatively, upon reacting with HCO, NO can be transformed by the BNC of other intermediates to form the nitrite-bound enzyme [71,88]. In this 'nitrite' pathway, NO is oxidized to nitrite by the **O** BNC in either slow or fast form, by **P**, and by **F** [29,31,70,71,112,113] (Figure 3). When encountering the fast HCO, NO initially interacts with the oxidized Cu_B rather than heme a_3, forming a Cu_B^+-NO^+ complex, which is subsequently hydroxylated to generate nitrite, a proton, and Cu_B^+ [108]. During the reaction, one electron is then made available at the BNC, allowing its re-equilibrating rapidly with heme *a* via reverse electron transfer. In the end, the heme a_3 nitrosyl complex is formed, and the enzyme is inhibited [108,114]. Inhibition of HCOs by NO through these 'nitrite' pathways, similar to the nitrosylation pathway, is reversible, and activity is restored by expelling nitrite from the heme a_3 nitrosyl complex [71,115].

Consistent with the independent discovery of these two pathways, they coexist upon NO exposure [29,40]. One pathway that prevails over the other depends on the turnover conditions and concentration of NO and physiological substrates, cytochrome *c* and O_2 [111]. When O_2 and NO are allowed to react at the same time with the enzyme, inhibition by NO may or may not occur in competition with O_2, depending on the fractional distribution of the catalytic intermediates of aa_3-HCO. Since Oxygen can only bind to the **R** BNC [116], which is the only intermediate that can react with both O_2 and NO, and the BNC in the states **O**, **E**, **P**, and **F** can solely react with NO, the reaction of NO with these latter intermediates does not occur in competition with O_2 [30,117–119].

Both pathways have been suggested to contribute to the resistance of *bd* QO to NO, although the molecular mechanism at the basis of inhibition of this enzyme by NO has not been fully elucidated [120]. Cu_B within HCOs plays an important role in determining the reaction rate with NO, and the NO dissociation rate from the nitrosyl adduct formed [41]. In the Cu-lacking *bd* QO, heme *b*-595 mimics the role of Cu_B in HCOs to react with NO at a rate that is remarkably slow compared to the HCO BNC, limiting nitrite production (via the 'nitrite' pathway) [114,120–122]. Moreover, although the *bd* enzyme also interacts with NO to form the nitrosyl adduct through the nitrosylation pathway, it has an NO dissociation rate substantially faster than that of HCOs [42,120,123]. The property results in prompt restoration of the enzyme activity with decreasing concentrations of NO. Interestingly, the mycobacterial *bcc-aa*$_3$ supercomplex is hyperresistant to NO inhibition (at 30 μM) more than other HCOs and even *bd* QO, which exhibit reduced activity in the presence of NO in the nanomolar range [42]. It is proposed that upon NO exposure, the newly formed nitrite by this *bcc-aa*$_3$ supercomplex may not bind to the heme a_3 moiety, presumably due to low affinity, and as a consequence, is expelled immediately from the enzyme without compromising oxygen reduction [94].

Similar to NO, nitrite also displays inhibitory effects on HCOs [22]. As nitrite can be transformed by a variety of proteins, including HCO, into other nitrogen oxides, especially NO, its inhibition has been attributed to NO for decades [124]. Thus, to date, investigations into the mechanisms underpinning the inhibition of HCOs by nitrite have been scarce. Nevertheless, in vitro biochemical analyses have demonstrated that the inhibitions of hemoproteins by the two molecules are not identical, albeit similar [125,126]. Although both NO and nitrite involve the formation of a ferrous-nitrosyl (Fe^{2+}-NO) complex upon binding to the ferrous ion within heme, leading to dissociation of the proximal histidine ligand [126], NO interacts with heme to directly form the Fe^{2+}-NO complex, whereas it is a two-step process for nitrite as nitrite has to be converted to NO first [20,36,127]. In recent years, new chemistries between nitrite and hemoproteins have been revealed [128]. Upon interaction of nitrite with hemoproteins, the iron-nitrosyl product is formed and subsequently enters a nitrite reductase/anhydrase redox pathway converting two molecules of nitrite into dinitrogen trioxide (N_2O_3) [129]. N_2O_3 may then nitrosate proteins and reconstitute NO via homolysis to NO and $NO_2^{\bullet}$. Meanwhile, nitrite is found to increase H_2O_2 levels by directly inhibiting catalase or reacting with hemoproteins under O_2 replete conditions to generate H_2O_2, introducing oxidative stress on cells [128,130]. Clearly, further studies are required to determine the contribution of the secondary effects induced by nitrite, including the N_2O_3 formation and the oxidative stress, to the inhibition of nitrite.

5. HCOs Are Primary Targets of Nitrite but Not NO In Vivo

Upon exposure to nitrite, the most evident phenotype of bacterial cells is impaired growth, which underlies the long history of using the nitrogen oxide as a preservative in meat products [131]. From earlier studies of growth inhibition by nitrite, two hypotheses have been proposed to explain the nature of the inhibition. In *Pseudomonas aeruginosa*, nitrite was initially found to inhibit active transport, oxygen uptake, and oxidative phosphorylation, thereby reducing aerobic respiration [39]. Later, it was demonstrated by in vitro analyses that nitrite directly compromises *cbb*$_3$-HCO of *P. aeruginosa* [39,132]. Such a phenomenon was not observed with bacteria without an HCO, such as *Clostridium* species, in which early investigations into the antimicrobial mechanism of nitrite were mostly conducted as the toxin produced from *Clostridium botulinum* is of particular concern in vacuum-packaged meat products [39]. Instead, it had been suggested in *Clostridium* species that the growth defect caused by nitrite is linked to pyruvate-ferredoxin oxidoreductase that carries a single Fe-S cluster, whose inactivation results in the accumulation of pyruvate [133,134]. Despite the lack of direct evidence, the inhibition of this enzyme by nitrite is proposed to be carried out by reaction of nitrite-derived NO rather than by nitrite per se [134]. The idea that nitrite inhibition depends on NO was boosted by the finding reported in 1983 that iron-sulfur proteins in vegetative cells of *C. botulinum* react with added nitrite

to form iron-NO complexes, with resultant destruction of the iron-sulfur cluster [124]. Ever since, it has been widely considered that the antibacterial effects of nitrite are attributable to NO formation.

Given that NO attracts all the attention, attempts aiming at identifying bacterial proteins susceptible to NO have been repeatedly made, especially with high-throughput screening approaches. Not surprisingly, a broad array of redox-active enzymes have been identified to be susceptible to NO, including aconitase, argininosuccinate synthase, dihydroxyacid dehydratase, fructose-1,6-biphosphate aldolase, pyruvate dehydrogenase, lipoamide dehydrogenase, and α-ketoglutarate dehydrogenase, most of which carry a Fe-S cluster (Figure 5) [28,135–139]. Importantly, NO targets associated with bacteriostasis differ significantly from one species to another, in some cases even within the same species, implying that the homeostasis of redox-sensitive proteins may largely underpin the substantial difference in NO-targets identified to date among different bacteria [138]. Unexpectedly, although HCOs and *bd* QOs have been individually identified to be NO-targets [42,123,140–142], they, even hemoproteins, were not among the identified in two comprehensive screenings of *E. coli* and *Salmonella enterica* serovar Typhimurium (*S.* Typhi), suggesting that they do not belong to the primary NO-target repertoire linked to the NO-caused growth arrest [137,138].

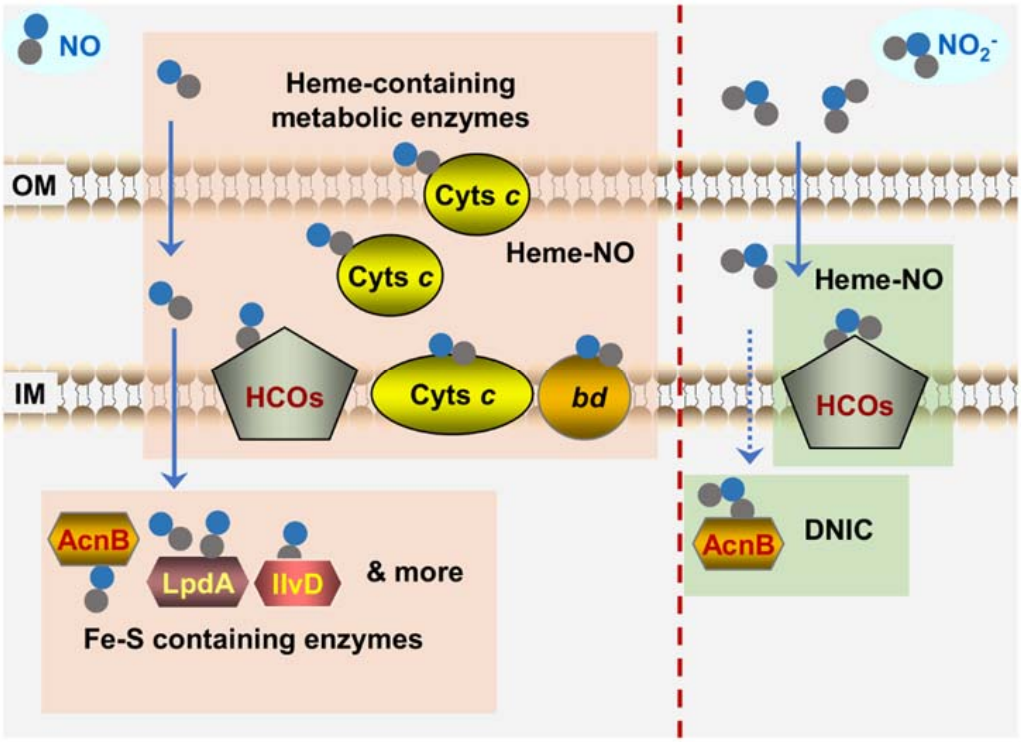

Figure 5. Bacterial targets of NO and nitrite revealed by in vivo analyses. Shown is the scenario that bacteria are confronted with NO from exogenous sources. The proteins sensitive to NO primarily include: (i) Fe-S containing dehydratases such as LpdA, IIvD, and AcnB that can form DNIC with NO; (ii) hemoproteins such as cyts c, HCOs, and cyt bd quinol oxidase that can form Fe^{2+}-NO complex. Unlike NO, the targets of nitrite are more specific. HCOs are the most crucial targets of nitrite. Besides, housekeeping aconitase AcnB rapidly loses activity upon nitrite exposure. Dashline arrow for the transport of nitrite represents that the molecules, unlike NO, could not diffuse into the cytoplasm easily. OM and IM represent outer- and inner-membrane of Gram-negative bacteria, respectively. Solid and dash line arrows represent crossing the membranes freely and in a transporter-dependent manner respectively.

However, a twist took place recently where cyts *c* have been identified to be crucial targets of NO in bacteria that are particularly rich in this type of protein, such as *Shewanella*

oneidensis, which is renowned for respiratory versatility largely owing to 42 different cyts *c* [143–145] (Figure 5). In vitro biochemical analyses have firmly established that cyts *c*, the same as other hemoproteins, are highly susceptible to both NO and nitrite, although they differ from them in that they contain one or several heme molecules through covalent linkages [36,146]. More importantly, as all cyts *c* are located exclusively outside the cytoplasm (either membrane-bound or soluble in the periplasm of Gram-negative bacteria), they are at the forefront of the attack by exogenous NO and nitrite. In *S. oneidensis*, the overall cyt *c* content rather than any individual cyt *c* dictates the susceptibility to NO because the loss of all cyts *c*, but not any single one of them, elicits a drastic difference in the sensitivity of the cells to NO (wild-type vs. cyt *c*-deficient strains) [147]. Moreover, the NO tolerance of *S. oneidensis* increases with the overall cyt *c* abundance that is manipulated by up-regulation of cyt *c* biosynthesis [147]. A similar scenario has been observed in *E. coli*, despite its relatively low cyt *c* abundance, which confers the cell's NO tolerance less effectively.

In cyt *c*-deficient mutants of *S. oneidensis*, metabolic enzymes were identified to be the NO targets in other bacteria that are critically linked to the impairment caused by NO growth, such as aconitase and dihydroxyacid dehydratase, become hypersensitive to NO [147] (Figure 5). Based on all of these findings, it has been proposed that cyts *c* appear to function as a major NO sink, especially in bacteria rich in such proteins, resulting in reduced intracellular levels of free NO and thus protecting other growth-critical targets. Since NO dissociation from the ferrous-nitrosyl (Fe^{2+}-NO) complexes is the rate-limiting process [36], this sinking effect is conceivably not likely to be very transient. Furthermore, this proposal offers one possible explanation for the failure that cyts *c* are not among the NO targets identified in *E. coli* and *S. Typhi* because they are not involved in aerobic growth, in which QOs (non-cyt *c* HCOs) are employed to respire oxygen [44].

In contrast to NO, HCOs are the specific and primary cellular target of nitrite. *S. oneidensis* and *E. coli* strains devoid of *bd* QO are highly sensitive to nitrite, whereas the loss of HCO (cbb_3-HCO and *bo*-HCO for *S. oneidensis* and *E. coli*, respectively) does not affect nitrite tolerance [148–150] (Figure 5). On the contrary, *bd* QO is dispensable to NO inhibition. When the cyt *c* contents are produced at similar levels, the presence of *bd* QO or not does not introduce a significant impact on growth [80,147,148,151]. These findings are in line with the properties of HCOs and *bd* QO revealed in in vitro analyses that the former are substantially more sensitive to nitrite than the latter in bacteria [42,152]. Moreover, the influence of cyts *c* on nitrite-induced bacteriostasis is negligible as the depletion of all cyts *c* only affects the susceptibility to NO but not to nitrite [147].

Further investigations into the NO-independent impacts of nitrite on HCOs have demonstrated that the essence of nitrite inhibition is proton translocation [153–156]. In *P. aeruginosa*, nitrite could not only prevent biofilm formation on the apical surface of airway epithelial cells but also modulate susceptibility to aminoglycosides by inhibiting bacterial respiration and oxygen uptake [157–159]. While HCOs and *bd* QOs differ from each other substantially in proton translocation efficiency, they appear similar in oxygen consumption [5,14,156]. A systematic survey of all types of HCOs with respect to their impacts on aminoglycoside susceptibility, including aa_3-HCO from *Bacillus subtilis* and *Staphylococcus aureus*, caa_3-HCO from *S. oneidensis*, cbb_3-HCO from *S. oneidensis* and *P. aeruginosa*, and bo_3-HCO from *E. coli*, have demonstrated that nitrite confers the cell's increased tolerance to a variety of aminoglycosides by inhibiting all of these HCOs under test [148,156]. This effect coincides with that caused by pmf destroyers CCCP and KCN, but is in contrast to that resulting from bedaquiline, which affects respiration (oxygen consumption) but not pmf. Thus, the mechanism underlying the modulation of aminoglycoside susceptibility by nitrite is to inhibit HCOs by abolishing proton translocation via proton pumping [153,156].

In addition to the NO-independent inhibition of HCOs by nitrite, recent advances have revealed an array of physiological aspects in which nitrite and NO function independently from each other. These include enzymes for their formation and detoxification and novel biological activities such as the lowing effect of nitrite on blood pressure [22,160]. In

addition, nitrite and NO as signal molecules at very low concentrations are perceived by completely different sensing systems, through which they are linked to different biological processes [22,161]. Moreover, in recent years, nitrite has been gradually rediscovered as a beneficial molecule, either endogenously formed or therapeutically added [162,163]. Nitrite (nebulized sodium nitrite) is currently in a phase 2b clinical trial as a drug for pulmonary hypertension treatment on the basis of the finding that it could be safely applied to reach millimolar concentrations in the airway surface liquid [164]. These findings from in vivo studies would undoubtedly, in turn, prompt more focused investigations into the mechanistic differences in the interactions of proteins to NO and nitrite.

6. Concluding Remarks

HCOs are transmembrane enzymes that catalyze the reduction of O_2 to H_2O, through which the energy is conserved as a proton gradient across the membrane via electrogenic chemistry and proton pumping. As redox-sensitive hemoproteins, HCOs readily interact with nitrogen oxides, nitrite, and NO in particular. While the interaction enables these enzymes to carry out biotransformation of nitrogen oxides, it also results in inhibition of catalytic activity. HCOs of eukaryotes are capable of reducing NO_2^- to NO, but most of their prokaryotic counterparts reduce NO to N_2O. Nevertheless, this reduction is not associated with proton pumping as it involves only one electron. Inhibition of HCOs by NO is rapid and reversible, which occurs in competition with oxygen only in the fully reduced state. In contrast, HCOs in the partially reduced and fully oxidized form can solely react with NO. Despite the lack of direct evidence, the inhibition of HCOs by nitrite is proposed to be via NO.

The importance of nitrite in the physiology of living organisms has gone unrecognized since the introduction of the notion that nitrite has effects through the formation of NO. Despite this, it is now clear that nitrite and NO are largely seen as two distinct nitrogen oxides by bacterial cells, although they share some common biochemical properties. NO appears to interact with most, if not all, redox-sensitive proteins, whereas nitrite shows high specificity. In particular, NO indiscriminately interacts with a variety of cytochromes *c*, presumably all hemoproteins, but nitrite inhibits HCOs specifically. Naturally, there must be mechanistic differences in the inactivation of HCOs by nitrite and NO. It should be noted that although bacterial HCOs share the common core architecture with more complex eukaryotic counterparts, they evolve through long-term adaptation, varying environments to possess distinctive features that allow them to exploit a much broader set of chemistries. However, compared to eukaryotic HCOs, structural and mechanistic studies to elucidate biochemical principles underlying the interaction between bacterial HCOs and nitrogen oxides remain limited, and are urgently needed.

In recent years, diverse and different solutions to respond and cope with nitrite and NO in bacteria have been revealed, relying on the sensory proteins that are extremely sensitive to changes in the concentrations of the chemicals. One may imagine that these sensors, mainly hemoproteins, can be exploited to address the mechanistic differences in interacting with nitrite and NO. More excitingly, in addition to NO, which has been administrated in clinical settings for decades, nitrite is now on the journey from toxin to therapy. It is, therefore, optimistic to predict that novel and surprising mechanisms, which reconcile the similar biochemical properties with the different physiological impacts of NO and nitrite, will be unraveled in living organisms, especially microorganisms, because they do not conform to boundaries.

Funding: This research was supported by the National Natural Science Foundation of China grants 31930003, 41976087, and 32100202, and Zhejiang Provincial Natural Science Foundation of China grant LR22C010001.

Conflicts of Interest: The authors declare no conflict of interest.

References

1. Verstraeten, N.; Knapen, W.J.; Kint, C.I.; Liebens, V.; Van den Bergh, B.; Dewachter, L.; Michiels, J.E.; Fu, Q.; David, C.C.; Fierro, A.C.; et al. Obg and membrane depolarization are part of a microbial bet-hedging strategy that leads to antibiotic tolerance. *Mol. Cell.* **2015**, *59*, 9–21. [CrossRef] [PubMed]
2. Wang, M.; Chan, E.W.C.; Wan, Y.; Wong, M.H.; Chen, S. Active maintenance of proton motive force mediates starvation-induced bacterial antibiotic tolerance in *Escherichia coli*. *Commun. Biol.* **2021**, *4*, 1068. [CrossRef] [PubMed]
3. Kaila, V.R.I.; Wikström, M. Architecture of bacterial respiratory chains. *Nat. Rev. Microbiol.* **2021**, *19*, 319–330. [CrossRef]
4. Sousa, F.L.; Alves, R.J.; Ribeiro, M.A.; Pereira-Leal, J.B.; Teixeira, M.; Pereira, M.M. The superfamily of heme-copper oxygen reductases: Types and evolutionary considerations. *Biochim. Biophys. Acta Bioenerg.* **2012**, *1817*, 629–637. [CrossRef]
5. Siletsky, S.A.; Borisov, V.B. Proton pumping and non-pumping terminal respiratory oxidases: Active sites intermediates of these molecular machines and their derivatives. *Int. J. Mol. Sci.* **2021**, *22*, 10852. [CrossRef]
6. Hemp, J.; Gennis, R.B. Diversity of the heme–copper superfamily in archaea: Insights from genomics and structural modeling. In *Bioenergetics: Energy Conservation and Conversion*; Schäfer, G., Penefsky, H.S., Eds.; Springer: Berlin/Heidelberg, Germany, 2008; Volume 45, pp. 1–31.
7. Wikström, M.; Krab, K.; Sharma, V. Oxygen activation and energy conservation by cytochrome *c* oxidase. *Chem. Rev.* **2018**, *118*, 2469–2490. [CrossRef]
8. Abramson, J.; Riistama, S.; Larsson, G.; Jasaitis, A.; Svensson-Ek, M.; Laakkonen, L.; Puustinen, A.; Iwata, S.; Wikström, M. The structure of the ubiquinol oxidase from *Escherichia coli* and its ubiquinone binding site. *Nat. Struct. Biol.* **2000**, *7*, 910–917. [PubMed]
9. Liu, J.; Hiser, C.; Ferguson-Miller, S. Role of conformational change and K-path ligands in controlling cytochrome *c* oxidase activity. *Biochem. Soc. Trans.* **2017**, *45*, 1087–1095. [CrossRef]
10. Lyons, J.A.; Aragão, D.; Slattery, O.; Pisliakov, A.V.; Soulimane, T.; Caffrey, M. Structural insights into electron transfer in caa_3-type cytochrome oxidase. *Nature* **2012**, *487*, 514–518. [CrossRef] [PubMed]
11. Buschmann, S.; Warkentin, E.; Xie, H.; Langer, J.D.; Ermler, U.; Michel, H. The structure of cbb_3 cytochrome oxidase provides insights into proton pumping. *Science* **2010**, *329*, 327–330. [CrossRef] [PubMed]
12. Faxén, K.; Gilderson, G.; Ädelroth, P.; Brzezinski, P. A mechanistic principle for proton pumping by cytochrome *c* oxidase. *Nature* **2005**, *437*, 286–289. [CrossRef]
13. Belevich, I.; Bloch, D.A.; Belevich, N.; Wikstrom, M.; Verkhovsky, M.I. Exploring the proton pump mechanism of cytochrome *c* oxidase in real time. *Proc. Natl. Acad. Sci. USA* **2007**, *104*, 2685–2690. [CrossRef]
14. Borisov, V.B.; Gennis, R.B.; Hemp, J.; Verkhovsky, M.I. The cytochrome *bd* respiratory oxygen reductases. *Biochim. Biophys. Acta Bioenerg.* **2011**, *1807*, 1398–1413. [CrossRef] [PubMed]
15. Safarian, S.; Rajendran, C.; Müller, H.; Preu, J.; Langer, J.D.; Ovchinnikov, S.; Hirose, T.; Kusumoto, T.; Sakamoto, J.; Michel, H. Structure of a *bd* oxidase indicates similar mechanisms for membrane-integrated oxygen reductases. *Science* **2016**, *352*, 583–586. [CrossRef] [PubMed]
16. Iwata, S.; Ostermeier, C.; Ludwig, B.; Michel, H. Structure at 2.8 A resolution of cytochrome *c* oxidase from *Paracoccus denitrificans*. *Nature* **1995**, *376*, 660–669. [CrossRef] [PubMed]
17. Yoshikawa, S.; Shimada, A. Reaction Mechanism of cytochrome *c* oxidase. *Chem. Rev.* **2015**, *115*, 1936–1989. [CrossRef] [PubMed]
18. Sharma, V.; Karlin, K.D.; Wikström, M. Computational study of the activated O(H) state in the catalytic mechanism of cytochrome *c* oxidase. *Proc. Natl. Acad. Sci. USA* **2013**, *110*, 16844–16849. [CrossRef] [PubMed]
19. Maia, L.B.; Moura, J.J. How biology handles nitrite. *Chem. Rev.* **2014**, *114*, 5273–5357. [CrossRef]
20. Canfield, D.E.; Glazer, A.N.; Falkowski, P.G. The evolution and future of earth's nitrogen cycle. *Science* **2010**, *330*, 192–196. [CrossRef] [PubMed]
21. Kuypers, M.M.M.; Marchant, H.K.; Kartal, B. The microbial nitrogen-cycling network. *Nat. Rev. Microbiol.* **2018**, *16*, 263–276. [CrossRef] [PubMed]
22. Guo, K.L.; Gao, H.C. Physiological roles of nitrite and nitric oxide in bacteria: Similar consequences from distinct cell targets, protection, and sensing systems. *Adv. Biol.* **2021**, *5*, e2100773. [CrossRef]
23. Jeney, V.; Ramos, S.; Bergman, M.-L.; Bechmann, I.; Tischer, J.; Ferreira, A.; Oliveira-Marques, V.; Janse, C.J.; Rebelo, S.; Cardoso, S.; et al. Control of disease tolerance to malaria by nitric oxide and carbon monoxide. *Cell Rep.* **2014**, *8*, 126–136. [CrossRef]
24. Mancuso, C.; Navarra, P.; Preziosi, P. Roles of nitric oxide, carbon monoxide, and hydrogen sulfide in the regulation of the hypothalamic–pituitary–adrenal axis. *J. Neurochem.* **2010**, *113*, 563–575. [CrossRef]
25. Mendes, S.S.; Miranda, V.; Saraiva, L.M. Hydrogen sulfide and carbon monoxide tolerance in bacteria. *Antioxidants* **2021**, *10*, 729. [CrossRef]
26. Moustafa, A. Changes in nitric oxide, carbon monoxide, hydrogen sulfide and male reproductive hormones in response to chronic restraint stress in rats. *Free Radic. Biol. Med.* **2021**, *162*, 353–366. [CrossRef]
27. Nowaczyk, A.; Kowalska, M.; Nowaczyk, J.; Grześk, G. Carbon monoxide and nitric oxide as examples of the youngest class of transmitters. *Int. J. Mol. Sci.* **2021**, *22*, 6029. [CrossRef]
28. Stern, A.M.; Zhu, J. An introduction to nitric oxide sensing and response in bacteria. *Adv. Appl. Microbiol.* **2014**, *87*, 187–220.

29. Brudvig, G.W.; Stevens, T.H.; Chan, S.I. Reactions of nitric-oxide with cytochrome-c oxidase. *Biochemistry* **1980**, *19*, 5275–5285. [CrossRef]
30. Sarti, P.; Forte, E.; Mastronicola, D.; Giuffrè, A.; Arese, M. Cytochrome *c* oxidase and nitric oxide in action: Molecular mechanisms and pathophysiological implications. *Biochim. Biophys. Acta Bioenerg.* **2012**, *1817*, 610–619. [CrossRef]
31. Sarti, P.; Giuffrè, A.; Barone, M.C.; Forte, E.; Mastronicola, D.; Brunori, M. Nitric oxide and cytochrome oxidase: Reaction mechanisms from the enzyme to the cell. *Free Radic. Biol. Med.* **2003**, *34*, 509–520. [CrossRef]
32. Hematian, S.; Siegler, M.A.; Karlin, K.D. Heme/Copper assembly mediated nitrite and nitric oxide interconversion. *J. Am. Chem. Soc.* **2012**, *134*, 18912–18915. [CrossRef]
33. Loullis, A.; Pinakoulaki, E. Probing the nitrite and nitric oxide reductase activity of cbb_3 oxidase: Resonance Raman detection of a six-coordinate ferrous heme–nitrosyl species in the binuclear b_3/CuB center. *Chem. Commun.* **2015**, *51*, 17398–17401. [CrossRef]
34. Giuffre, A.; Stubauer, G.; Sarti, P.; Brunori, M.; Zumft, W.G.; Buse, G.; Soulimane, T. The heme-copper oxidases of *Thermus thermophilus* catalyze the reduction of nitric oxide: Evolutionary implications. *Proc. Natl. Acad. Sci. USA* **1999**, *96*, 14718–14723. [CrossRef]
35. Castello, P.R.; David, P.S.; McClure, T.; Crook, Z.; Poyton, R.O. Mitochondrial cytochrome oxidase produces nitric oxide under hypoxic conditions: Implications for oxygen sensing and hypoxic signaling in eukaryotes. *Cell Metab.* **2006**, *3*, 277–287. [CrossRef]
36. Ford, P.C. Reactions of NO and nitrite with heme models and proteins. *Inorg. Chem.* **2010**, *49*, 6226–6239. [CrossRef]
37. Ford, P.C.; Miranda, K.M. The solution chemistry of nitric oxide and other reactive nitrogen species. *Nitric Oxide* **2020**, *103*, 31–46. [CrossRef]
38. Yoshikawa, S.; Orii, Y. Inhibition mechanism of cytochrome-oxidase reaction 2 classifications of inhibitors based on their modes of action. *J. Biochem.* **1972**, *71*, 859–872. [CrossRef]
39. Rowe, J.J.; Yarbrough, J.M.; Rake, J.B.; Eagon, R.G. Nitrite inhibition of aerobic-bacteria. *Curr. Microbiol.* **1979**, *2*, 51–54. [CrossRef]
40. Stevens, T.H.; Brudvig, G.W.; Bocian, D.F.; Chan, S.I. Structure of cytochrome a_3-CuA_3 couple in cytochrome *c* oxidase as revealed by nitric oxide binding studies. *Proc. Natl. Acad. Sci. USA* **1979**, *76*, 3320–3324. [CrossRef]
41. Hori, H.; Tsubaki, M.; Mogi, T.; Anraku, Y. EPR study of NO complexes of bd-type ubiquinol oxidase from *Escherichia coli*: The proximal axial ligand of heme D is a nitrogenous amino acid residue. *J. Biol. Chem.* **1996**, *271*, 9254–9258. [CrossRef]
42. Mason, M.G.; Shepherd, M.; Nicholls, P.; Dobbin, P.S.; Dodsworth, K.S.; Poole, R.K.; Cooper, C.E. Cytochrome *bd* confers nitric oxide resistance to *Escherichia coli*. *Nat. Chem. Biol.* **2009**, *5*, 94–96. [CrossRef]
43. Lyons, J.A.; Hilbers, F.; Caffrey, M. Structure and function of bacterial cytochrome *c* oxidases. In *Cytochrome Complexes: Evolution, Structures, Energy Transduction, and Signaling*; Cramer, W.A., Kallas, T., Eds.; Advances in Photosynthesis and Respiration; Springer: Dordrecht, The Netherlands, 2016; Volume 41, pp. 307–329.
44. Wikström, M.; Verkhovsky, M.I. Mechanism and energetics of proton translocation by the respiratory heme-copper oxidases. *Biochim. Biophys. Acta Bioenerg.* **2007**, *1767*, 1200–1214. [CrossRef]
45. Lu, Y.; Sigman, J.A.; Kim, H.K.; Zhao, X.; Carey, J.R. The role of copper and protons in heme-copper oxidases: Kinetic study of an engineered heme-copper center in myoglobin. *J. Inorg. Biochem.* **2003**, *96*, 183. [CrossRef]
46. Giuffrè, A.; Borisov, V.B.; Arese, M.; Sarti, P.; Forte, E. Cytochrome *bd* oxidase and bacterial tolerance to oxidative and nitrosative stress. *Biochim. Biophys. Acta Bioenerg.* **2014**, *1837*, 1178–1187. [CrossRef]
47. Borisov, V.B.; Forte, E. Terminal oxidase cytochrome *bd* protects bacteria against hydrogen sulfide toxicity. *Biochemistry* **2021**, *86*, 22–32. [CrossRef]
48. Borisov, V.B.; Siletsky, S.A.; Nastasi, M.R.; Forte, E. ROS defense systems and terminal oxidases in bacteria. *Antioxidants* **2021**, *10*, 839. [CrossRef]
49. Korshunov, S.; Imlay, K.R.; Imlay, J.A. The cytochrome *bd* oxidase of *Escherichia coli* prevents respiratory inhibition by endogenous and exogenous hydrogen sulfide. *Mol. Microbiol.* **2016**, *101*, 62–77. [CrossRef]
50. Yoshikawa, S.; Muramoto, K.; Shinzawa-Itoh, K. Proton-pumping mechanism of cytochrome *c* oxidase. *Annu. Rev. Biophys.* **2011**, *40*, 205–223. [CrossRef]
51. Pereira, M.M.; Santana, M.; Teixeira, M. A novel scenario for the evolution of haem-copper oxygen reductases. *Biochim. Biophys. Acta Bioenerg.* **2001**, *1505*, 185–208. [CrossRef]
52. Florens, L.; Schmidt, B.; McCracken, J.; Ferguson-Miller, S. Fast deuterium access to the buried magnesium/manganese site in cytochrome *c* oxidase. *Biochemistry* **2001**, *40*, 7491–7497. [CrossRef]
53. Mills, D.A.; Florens, L.; Hiser, C.; Qian, J.; Ferguson-Miller, S. Where is ′outside′ in cytochrome *c* oxidase and how and when do protons get there? *Biochim. Biophys. Acta Bioenerg.* **2000**, *1458*, 180–187. [CrossRef]
54. Soulimane, T.; Buse, G.; Bourenkov, G.P.; Bartunik, H.D.; Huber, R.; Than, M.E. Structure and mechanism of the aberrant $ba_{(3)}$-cytochrome *c* oxidase from *thermus thermophilus*. *EMBO J.* **2000**, *19*, 1766–1776. [CrossRef] [PubMed]
55. Zhu, G.; Zeng, H.; Zhang, S.; Juli, J.; Tai, L.; Zhang, D.; Pang, X.; Zhang, Y.; Lam, S.M.; Zhu, Y.; et al. The unusual homodimer of a heme-copper terminal oxidase allows itself to utilize two electron donors. *Angew. Chem. Int. Ed.* **2021**, *60*, 13323–13330. [CrossRef]
56. Pinakoulaki, E.; Stavrakis, S.; Urbani, A.; Varotsis, C. Resonance Raman Detection of a Ferrous Five-Coordinate Nitrosylheme b_3 Complex in Cytochrome cbb_3 Oxidase from *Pseudomonas stutzeri*. *J. Am. Chem. Soc.* **2002**, *124*, 9378–9379. [CrossRef] [PubMed]

57. Kohlstaedt, M.; Buschmann, S.; Langer, J.D.; Xie, H.; Michel, H. Subunit CcoQ is involved in the assembly of the $cbb_{(3)}$-type cytochrome *c* oxidases from *Pseudomonas stutzeri* ZoBell but not required for their activity. *Biochim. Biophys. Acta Bioenerg.* **2017**, *1858*, 231–238. [CrossRef] [PubMed]
58. Agmon, N. The grotthuss mechanism. *Chem. Phys. Lett.* **1995**, *244*, 456–462. [CrossRef]
59. Harrenga, A.; Michel, H. The cytochrome *c* oxidase from *Paracoccus denitrificans* does not change the metal center ligation upon reduction. *J. Biol. Chem.* **1999**, *274*, 33296–33299. [CrossRef] [PubMed]
60. Kim, Y.C.; Wikström, M.; Hummer, G. Kinetic gating of the proton pump in cytochrome *c* oxidase. *Proc. Natl. Acad. Sci. USA* **2009**, *106*, 13707–13712. [CrossRef] [PubMed]
61. Pereira, M.M.; Santana, M.; Soares, C.M.; Mendes, J.; Carita, J.N.; Fernandes, A.S.; Saraste, M.; Carrondo, M.A.; Teixeira, M. The caa_3 terminal oxidase of the thermohalophilic bacterium *Rhodothermus marinus*: A HiPIP:oxygen oxidoreductase lacking the key glutamate of the D-channel. *Biochim. Biophys. Acta Bioenerg.* **1999**, *1413*, 1–13. [CrossRef]
62. Qin, L.; Mills, D.A.; Buhrow, L.; Hiser, C.; Ferguson-Miller, S. A conserved steroid binding site in cytochrome *c* oxidase. *Biochemistry* **2008**, *47*, 9931–9933. [CrossRef]
63. Hiser, C.; Buhrow, L.; Liu, J.; Kuhn, L.; Ferguson-Miller, S. A conserved amphipathic ligand binding region influences k-path-dependent activity of cytochrome *c* oxidase. *Biochemistry* **2013**, *52*, 1385–1396. [CrossRef]
64. Rauhamäki, V.; Baumann, M.; Soliymani, R.; Puustinen, A.; Wikström, M. Identification of a histidine-tyrosine cross-link in the active site of the *cbb3*-type cytochrome *c* oxidase from *Rhodobacter sphaeroides*. *Proc. Natl. Acad. Sci. USA* **2006**, *103*, 16135–16140. [CrossRef] [PubMed]
65. Drosou, V.; Malatesta, F.; Ludwig, B. Mutations in the docking site for cytochrome *c* on the *Paracoccus* heme aa_3 oxidase. Electron entry and kinetic phases of the reaction. *Eur. J. Biochem.* **2002**, *269*, 2980–2988. [CrossRef] [PubMed]
66. Muresanu, L.; Pristovsek, P.; Löhr, F.; Maneg, O.; Mukrasch, M.D.; Rüterjans, H.; Ludwig, B.; Lücke, C. The electron transfer complex between cytochrome c_{552} and the CuA domain of the *Thermus thermophilus* ba_3 oxidase. A combined NMR and computational approach. *J. Biol. Chem.* **2006**, *281*, 14503–14513. [CrossRef] [PubMed]
67. Gray, H.B. Electron flow through metalloproteins. *J. Inorg. Biochem.* **2001**, *86*, 1. [CrossRef]
68. Maneg, O.; Malatesta, F.; Ludwig, B.; Drosou, V. Interaction of cytochrome *c* with cytochrome oxidase: Two different docking scenarios. *Biochim. Biophys. Acta Bioenerg.* **2004**, *1655*, 274–281. [CrossRef]
69. Chance, B.; Saronio, C.; Leigh, J.S., Jr. Functional intermediates in the reaction of membrane-bound cytochrome oxidase with oxygen. *J. Biol. Chem.* **1975**, *250*, 9226–9237. [CrossRef]
70. Fabian, M.; Wong, W.W.; Gennis, R.B.; Palmer, G. Mass spectrometric determination of dioxygen bond splitting in the "peroxy" intermediate of cytochrome c oxidase. *Proc. Natl. Acad. Sci. USA* **1999**, *96*, 13114–13117. [CrossRef]
71. Giuffrè, A.; Barone, M.C.; Mastronicola, D.; D'Itri, E.; Sarti, P.; Brunori, M. Reaction of nitric oxide with the turnover intermediates of cytochrome *c* oxidase: Reaction pathway and functional effects. *Biochemistry* **2000**, *39*, 15446–15453. [CrossRef] [PubMed]
72. Blomberg, M.R.A. Activation of $O_{(2)}$ and NO in heme-copper oxidases—Mechanistic insights from computational modelling. *Chem. Soc. Rev.* **2020**, *49*, 7301–7330. [CrossRef]
73. Michel, H. Cytochrome *c* oxidase: Catalytic cycle and mechanisms of proton pumping—A discussion. *Biochemistry* **1999**, *38*, 15129–15140. [CrossRef] [PubMed]
74. Kaila, V.R.; Sharma, V.; Wikström, M. The identity of the transient proton loading site of the proton-pumping mechanism of cytochrome *c* oxidase. *Biochim. Biophys. Acta Bioenerg.* **2011**, *1807*, 80–84. [CrossRef]
75. Kaila, V.R.; Johansson, M.P.; Sundholm, D.; Laakkonen, L.; Wiström, M. The chemistry of the CuB site in cytochrome *c* oxidase and the importance of its unique His-Tyr bond. *Biochim. Biophys. Acta Bioenerg.* **2009**, *1787*, 221–233. [CrossRef] [PubMed]
76. Murali, R.; Gennis, R.B.; Hemp, J. Evolution of the cytochrome *bd* oxygen reductase superfamily and the function of CydAA′ in Archaea. *ISME J.* **2021**, *15*, 3534–3548. [CrossRef] [PubMed]
77. Azarkina, N.; Siletsky, S.; Borisov, V.; von Wachenfeldt, C.; Hederstedt, L.; Konstantinov, A.A. A cytochrome *bb′*-type quinol oxidase in *Bacillus subtilis* strain 168. *J. Biol. Chem.* **1999**, *274*, 32810–32817. [CrossRef]
78. Williams, C.; McColl, K.E. Review article: Proton pump inhibitors and bacterial overgrowth. *Aliment. Pharmacol. Ther.* **2006**, *23*, 3–10. [CrossRef]
79. Hoeser, J.; Hong, S.; Gehmann, G.; Gennis, R.B.; Friedrich, T. Subunit CydX of *Escherichia coli* cytochrome *bd* ubiquinol oxidase is essential for assembly and stability of the di-heme active site. *FEBS Lett.* **2014**, *588*, 1537–1541. [CrossRef]
80. Chen, H.; Luo, Q.; Yin, J.; Gao, T.; Gao, H. Evidence for the requirement of CydX in function but not assembly of the cytochrome *bd* oxidase in *Shewanella oneidensis*. *Biochim. Biophys. Acta Gen. Subj.* **2015**, *1850*, 318–328. [CrossRef]
81. Thesseling, A.; Rasmussen, T.; Burschel, S.; Wohlwend, D.; Kaegi, J.; Mueller, R.; Boettcher, B.; Friedrich, T. Homologous *bd* oxidases share the same architecture but differ in mechanism. *Nat. Commun.* **2019**, *10*, 5138. [CrossRef]
82. Osborne, J.P.; Gennis, R.B. Sequence analysis of cytochrome *bd* oxidase suggests a revised topology for subunit I. *Biochim. Biophys. Acta Bioenerg.* **1999**, *1410*, 32–50. [CrossRef]
83. Bertsova, Y.V.; Bogachev, A.V.; Skulachev, V.P. Generation of protonic potential by the *bd*-type quinol oxidase of *Azotobacter vinelandii*. *FEBS Lett.* **1997**, *414*, 369–372.
84. Forte, E.; Urbani, A.; Saraste, M.; Sarti, P.; Brunori, M.; Giuffrè, A. The cytochrome cbb_3 from *Pseudomonas stutzeri* displays nitric oxide reductase activity. *Eur. J. Biochem.* **2001**, *268*, 6486–6491. [CrossRef] [PubMed]

85. Butler, C.S.; Forte, E.; Maria Scandurra, F.; Arese, M.; Giuffré, A.; Greenwood, C.; Sarti, P. Cytochrome bo_3 from *Escherichia coli*: The binding and turnover of nitric oxide. *Biochem. Biophys. Res. Commun.* **2002**, *296*, 1272–1278. [CrossRef]
86. Hematian, S.; Garcia-Bosch, I.; Karlin, K.D. Synthetic heme/copper assemblies: Toward an understanding of cytochrome *c* oxidase interactions with dioxygen and nitrogen oxides. *Acc. Chem. Res.* **2015**, *48*, 2462–2474. [CrossRef]
87. Hematian, S.; Kenkel, I.; Shubina, T.E.; Dürr, M.; Liu, J.J.; Siegler, M.A.; Ivanovic-Burmazovic, I.; Karlin, K.D. Nitrogen oxide atom-transfer redox chemistry; mechanism of NO(g) to nitrite conversion utilizing μ-oxo Heme-FeIII–O–CuII(L) constructs. *J. Am. Chem. Soc.* **2015**, *137*, 6602–6615. [CrossRef]
88. Torres, J.; Cooper, C.E.; Wilson, M.T. A common mechanism for the interaction of nitric oxide with the oxidized binuclear centre and oxygen intermediates of cytochromec oxidase. *J. Biol. Chem.* **1998**, *273*, 8756–8766. [CrossRef]
89. Loullis, A.; Noor, M.R.; Soulimane, T.; Pinakoulaki, E. The structure of a ferrous heme-nitro species in the binuclear heme a_3/Cu_B center of ba_3-cytochrome *c* oxidase as determined by resonance Raman spectroscopy. *Chem. Commun.* **2015**, *51*, 286–289. [CrossRef] [PubMed]
90. Pinakoulaki, E.; Ohta, T.; Soulimane, T.; Kitagawa, T.; Varotsis, C. Detection of the His-Heme $Fe^{2+}-NO$ species in the reduction of NO to N_2O by ba_3-oxidase from *Thermus thermophilus*. *J. Am. Chem. Soc.* **2005**, *127*, 15161–15167. [CrossRef]
91. Daskalakis, V.; Ohta, T.; Kitagawa, T.; Varotsis, C. Structure and properties of the catalytic site of nitric oxide reductase at ambient temperature. *Biochim. Biophys. Acta Bioenerg.* **2015**, *1847*, 1240–1244. [CrossRef] [PubMed]
92. Ohta, T.; Soulimane, T.; Kitagawa, T.; Varotsis, C. Nitric oxide activation by caa_3 oxidoreductase from *Thermus thermophilus*. *Phys. Chem. Chem. Phys.* **2015**, *17*, 10894–10898. [CrossRef]
93. Varotsis, C.; Ohta, T.; Kitagawa, T.; Soulimane, T.; Pinakoulaki, E. The structure of the hyponitrite species in a heme Fe-Cu binuclear center. *Angew. Chem. Int. Ed.* **2007**, *46*, 2210–2214. [CrossRef]
94. Forte, E.; Giuffrè, A.; Huang, L.-s.; Berry, E.A.; Borisov, V.B. Nitric oxide does not inhibit but is metabolized by the cytochrome *bcc-aa*$_3$ supercomplex. *Int. J. Mol. Sci.* **2020**, *21*, 8521. [CrossRef]
95. Girsch, P.; de Vries, S. Purification and initial kinetic and spectroscopic characterization of NO reductase from *Paracoccus denitrificans*. *Biochim. Biophys. Acta Bioenerg.* **1997**, *1318*, 202–216. [CrossRef]
96. Hasenoehrl, E.J.; Wiggins, T.J.; Berney, M. Bioenergetic inhibitors: Antibiotic efficacy and mechanisms of action in *Mycobacterium tuberculosis*. *Front. Cell. Infect. Microbiol.* **2021**, *10*, 611683. [CrossRef] [PubMed]
97. Oliva, C.R.; Markert, T.; Ross, L.J.; White, E.L.; Rasmussen, L.; Zhang, W.; Everts, M.; Moellering, D.R.; Bailey, S.M.; Suto, M.J.; et al. Identification of small molecule inhibitors of human cytochrome *c* oxidase that target chemoresistant glioma cells. *J. Biol. Chem.* **2016**, *291*, 24188–24199. [CrossRef] [PubMed]
98. Pinakoulaki, E.; Vamvouka, M.; Varotsis, C. Resonance Raman detection of the $Fe^{2+}-C-N$ Modes in heme−copper oxidases: a probe of the active site. *Inorg. Chem.* **2004**, *43*, 4907–4910. [CrossRef] [PubMed]
99. Shimada, A.; Hatano, K.; Tadehara, H.; Yano, N.; Shinzawa-Itoh, K.; Yamashita, E.; Muramoto, K.; Tsukihara, T.; Yoshikawa, S. X-ray structural analyses of azide-bound cytochrome *c* oxidases reveal that the H-pathway is critically important for the proton-pumping activity. *J. Biol. Chem.* **2018**, *293*, 14868–14879. [CrossRef]
100. Alleyne, T.; Ignacio, D.N.; Sampson, V.B.; Ashe, D.; Wilson, M. Simulating the slow to fast switch in cytochrome *c* oxidase catalysis by introducing a loop flip near the enzyme′s cytochrome *c* (substrate) binding site. *Biotechnol. Appl. Biochem.* **2017**, *64*, 677–685. [CrossRef]
101. Moody, A.J.; Cooper, C.E.; Rich, P.R. Characterisation of 'fast' and 'slow' forms of bovine heart cytochrome-c oxidase. *Biochim. Biophys. Acta Bioenerg.* **1991**, *1059*, 189–207. [CrossRef]
102. Bloch, D.; Belevich, I.; Jasaitis, A.; Ribacka, C.; Puustinen, A.; Verkhovsky, M.I.; Wikström, M. The catalytic cycle of cytochrome *c* oxidase is not the sum of its two halves. *Proc. Natl. Acad. Sci. USA* **2004**, *101*, 529–533. [CrossRef]
103. Andersson, R.; Safari, C.; Dods, R.; Nango, E.; Tanaka, R.; Yamashita, A.; Nakane, T.; Tono, K.; Joti, Y.; Båth, P.; et al. Serial femtosecond crystallography structure of cytochrome *c* oxidase at room temperature. *Sci. Rep.* **2017**, *7*, 4518. [CrossRef]
104. Aoyama, H.; Muramoto, K.; Shinzawa-Itoh, K.; Hirata, K.; Yamashita, E.; Tsukihara, T.; Ogura, T.; Yoshikawa, S. A peroxide bridge between Fe and Cu ions in the O_2 reduction site of fully oxidized cytochrome *c* oxidase could suppress the proton pump. *Proc. Natl. Acad. Sci. USA* **2009**, *106*, 2165–2169. [CrossRef]
105. Koepke, J.; Olkhova, E.; Angerer, H.; Müller, H.; Peng, G.; Michel, H. High resolution crystal structure of *Paracoccus denitrificans* cytochrome *c* oxidase: New insights into the active site and the proton transfer pathways. *Biochim. Biophys. Acta Bioenerg.* **2009**, *1787*, 635–645. [CrossRef]
106. Kruse, F.; Nguyen, A.D.; Dragelj, J.; Heberle, J.; Hildebrandt, P.; Mroginski, M.A.; Weidinger, I.M. A Resonance Raman marker band characterizes the slow and fast form of cytochrome *c* oxidase. *J. Am. Chem. Soc.* **2021**, *143*, 2769–2776. [CrossRef] [PubMed]
107. Thörnström, P.-E.; Nilsson, T.; Malmström, B.G. The possible role of the closed-open transition in proton pumping by cytochrome *c* oxidase: The pH dependence of cyanide inhibition. *Biochim. Biophys. Acta Bioenerg.* **1988**, *935*, 103–108. [CrossRef]
108. Cooper, C.E.; Torres, J.; Sharpe, M.A.; Wilson, M.T. Nitric oxide ejects electrons from the binuclear centre of cytochrome *c* oxidase by reacting with oxidised copper: A general mechanism for the interaction of copper proteins with nitric oxide? *FEBS Lett.* **1997**, *414*, 281–284.
109. Muramoto, K.; Ohta, K.; Shinzawa-Itoh, K.; Kanda, K.; Taniguchi, M.; Nabekura, H.; Yamashita, E.; Tsukihara, T.; Yoshikawa, S. Bovine cytochrome *c* oxidase structures enable O_2 reduction with minimization of reactive oxygens and provide a proton-pumping gate. *Proc. Natl. Acad. Sci. USA* **2010**, *107*, 7740–7745. [CrossRef]

110. Stubauer, G.; Giuffrè, A.; Brunori, M.; Sarti, P. Cytochrome *c* oxidase does not catalyze the anaerobic reduction of NO. *Biochem. Biophys. Res. Commun.* **1998**, *245*, 459–465. [CrossRef]
111. Sarti, P.; Giuffré, A.; Forte, E.; Mastronicola, D.; Barone, M.C.; Brunori, M. Nitric oxide and cytochrome *c* oxidase: Mechanisms of inhibition and no degradation. *Biochem. Biophys. Res. Commun.* **2000**, *274*, 183–187. [CrossRef]
112. Antonini, E.; Brunori, M.; Colosimo, A.; Greenwood, C.; Wilson, M.T. Oxygen 'pulsed' cytochrome *c* oxidase: Functional properties and catalytic relevance. *Proc. Natl. Acad. Sci. USA* **1977**, *74*, 3128–3132. [CrossRef]
113. Baker, G.M.; Noguchi, M.; Palmer, G. The reaction of cytochrome oxidase with cyanide. Preparation of the rapidly reacting form and its conversion to the slowly reacting form. *J. Biol. Chem.* **1987**, *262*, 595–604. [CrossRef]
114. Giuffrè, A.; Stubauer, G.; Brunori, M.; Sarti, P.; Torres, J.; Wilson, M.T. Chloride bound to oxidized cytochrome *c* oxidase controls the reaction with nitric oxide. *J. Biol. Chem.* **1998**, *273*, 32475–32478. [CrossRef] [PubMed]
115. Antunes, F.; Cadenas, E. The mechanism of cytochrome *C* oxidase inhibition by nitric oxide. *Front. Biosci.* **2007**, *12*, 975–985. [CrossRef] [PubMed]
116. Sarti, P.; Arese, M.; Forte, E.; Giuffrè, A.; Mastronicola, D. Mitochondria and Nitric oxide: Chemistry and pathophysiology. In *Advances in Mitochondrial Medicine*; Scatena, R., Bottoni, P., Giardina, B., Eds.; Springer: Dordrecht, The Netherlands, 2012; pp. 75–92.
117. Mason, M.G.; Nicholls, P.; Wilson, M.T.; Cooper, C.E. Nitric oxide inhibition of respiration involves both competitive (heme) and noncompetitive (copper) binding to cytochrome *c* oxidase. *Proc. Natl. Acad. Sci. USA* **2006**, *103*, 708–713. [CrossRef]
118. Moncada, S.; Erusalimsky, J.D. Does nitric oxide modulate mitochondrial energy generation and apoptosis? *Nat. Rev. Mol. Cell Biol.* **2002**, *3*, 214–220. [CrossRef]
119. Ford, P.C.; Wink, D.A.; Stanbury, D.M. Autoxidation kinetics of aqueous nitric-oxide. *FEBS Lett.* **1993**, *326*, 1–3. [CrossRef]
120. Borisov, V.B.; Forte, E.; Sarti, P.; Brunori, M.; Konstantinov, A.A.; Giuffrè, A. Redox control of fast ligand dissociation from *Escherichia coli* cytochrome *bd*. *Biochem. Biophys. Res. Commun.* **2007**, *355*, 97–102. [CrossRef]
121. Borisov, V.B.; Forte, E.; Giuffrè, A.; Konstantinov, A.; Sarti, P. Reaction of nitric oxide with the oxidized di-heme and heme–copper oxygen-reducing centers of terminal oxidases: Different reaction pathways and end-products. *J. Inorg. Biochem.* **2009**, *103*, 1185–1187. [CrossRef]
122. Ohta, K.; Muramoto, K.; Shinzawa-Itoh, K.; Yamashita, E.; Yoshikawa, S.; Tsukihara, T. X-ray structure of the NO-bound CuB in bovine cytochrome *c* oxidase. *Acta Crystallogr. Sect. F Struct. Biol. Cryst. Commun.* **2010**, *66*, 251–253. [CrossRef]
123. Borisov, V.B.; Forte, E.; Konstantinov, A.A.; Poole, R.K.; Sarti, P.; Giuffrè, A. Interaction of the bacterial terminal oxidase cytochrome *bd* with nitric oxide. *FEBS Lett.* **2004**, *576*, 201–204. [CrossRef]
124. Reddy, D.; Lancaster, J.R., Jr.; Cornforth, D.P. Nitrite inhibition of *Clostridium botulinum: Electron* spin resonance detection of iron-nitric oxide complexes. *Science* **1983**, *221*, 769–770. [CrossRef]
125. Tonzetich, Z.J.; McQuade, L.E.; Lippard, S.J. Detecting and understanding the roles of nitric oxide in biology. *Inorg. Chem.* **2010**, *49*, 6338–6348. [CrossRef]
126. Xu, N.; Yi, J.; Richter-Addo, G.B. Linkage isomerization in heme-NO_x compounds: Understanding NO, nitrite, and hyponitrite interactions with iron porphyrins. *Inorg. Chem.* **2010**, *49*, 6253–6266. [CrossRef] [PubMed]
127. Gladwin, M.T.; Grubina, R.; Doyle, M.P. The new chemical biology of nitrite reactions with hemoglobin: R-state catalysis, oxidative denitrosylation, and nitrite reductase/anhydrase. *Acc. Chem. Res.* **2009**, *42*, 157–167. [CrossRef] [PubMed]
128. Dent, M.R.; DeMartino, A.W.; Tejero, J.; Gladwin, M.T. Endogenous hemoprotein-dependent signaling pathways of nitric oxide and nitrite. *Inorg. Chem.* **2021**, *60*, 15918–15940. [CrossRef] [PubMed]
129. Basu, S.; Grubina, R.; Huang, J.; Conradie, J.; Huang, Z.; Jeffers, A.; Jiang, A.; He, X.; Azarov, I.; Seibert, R.; et al. Catalytic generation of N_2O_3 by the concerted nitrite reductase and anhydrase activity of hemoglobin. *Nat. Chem. Biol.* **2007**, *3*, 785–794. [CrossRef]
130. Keszler, A.; Piknova, B.; Schechter, A.N.; Hogg, N. The reaction between nitrite and oxyhemoglobin: A mechanistic study. *J. Biol. Chem.* **2008**, *283*, 9615–9622. [CrossRef]
131. Tompkin, R. Nitrite. In *Antimicrobials in Food*, 3rd ed.; Davidson, P., Sofos, J., Branen, A., Eds.; CRC Press, Taylor&Frances Group: Boca Raton, FL, USA, 2005; pp. 169–236.
132. Yang, T.Y. Mechanism of nitrite inhibition of cellular respiration in *Pseudomonas aeruginosa*. *Curr. Microbiol.* **1985**, *12*, 35–39. [CrossRef]
133. Chabrière, E.; Charon, M.H.; Volbeda, A.; Pieulle, L.; Hatchikian, E.C.; Fontecilla-Camps, J.C. Crystal structures of the key anaerobic enzyme pyruvate: Ferredoxin oxidoreductase, free and in complex with pyruvate. *Nat. Struct. Biol.* **1999**, *6*, 182–190.
134. Woods, L.F.; Wood, J.M. A note on the effect of nitrite inhibition on the metabolism of *Clostridium botulinum*. *J. Appl. Bacteriol.* **1982**, *52*, 109–110. [CrossRef]
135. Bourret, T.J.; Boylan, J.A.; Lawrence, K.A.; Gherardini, F.C. Nitrosative damage to free and zinc-bound cysteine thiols underlies nitric oxide toxicity in wild-type *Borrelia burgdorferi*. *Mol. Microbiol.* **2011**, *81*, 259–273. [CrossRef]
136. Husain, M.; Bourret, T.J.; McCollister, B.D.; Jones-Carson, J.; Laughlin, J.; Vázquez-Torres, A. Nitric oxide evokes an adaptive response to oxidative stress by arresting respiration. *J. Biol. Chem.* **2008**, *283*, 7682–7689. [CrossRef] [PubMed]

137. Hyduke, D.R.; Jarboe, L.R.; Tran, L.M.; Chou, K.J.; Liao, J.C. Integrated network analysis identifies nitric oxide response networks and dihydroxyacid dehydratase as a crucial target in *Escherichia coli*. *Proc. Natl. Acad. Sci. USA* **2007**, *104*, 8484–8489. [CrossRef]
138. Richardson, A.R.; Payne, E.C.; Younger, N.; Karlinsey, J.E.; Thomas, V.C.; Becker, L.A.; Navarre, W.W.; Castor, M.E.; Libby, S.J.; Fang, F.C. Multiple targets of nitric oxide in the tricarboxylic acid cycle of *Salmonella enterica* serovar typhimurium. *Cell Host Microbe* **2011**, *10*, 33–43. [CrossRef]
139. Vine, C.E.; Cole, J.A. Unresolved sources, sinks, and pathways for the recovery of enteric bacteria from nitrosative stress. *FEMS Microbiol. Lett.* **2011**, *325*, 99–107. [CrossRef] [PubMed]
140. Butler, C.S.; Seward, H.E.; Greenwood, C.; Thomson, A.J. Fast cytochrome *bo* from *Escherichia coli* binds two molecules of nitric oxide at CuB. *Biochemistry* **1997**, *36*, 16259–16266. [CrossRef]
141. Giuffre, A.; Forte, E.; Brunori, M.; Sarti, P. Nitric oxide, cytochrome *c* oxidase and myoglobin: Competition and reaction pathways. *FEBS Lett.* **2005**, *579*, 2528–2532. [CrossRef]
142. Jones-Carson, J.; Husain, M.; Liu, L.; Orlicky, D.J.; Vázquez-Torres, A. Cytochrome *bd*-dependent bioenergetics and antinitrosative defenses in *Salmonella* pathogenesis. *mBio* **2016**, *7*, e02052-16. [CrossRef]
143. Meyer, T.E.; Tsapin, A.I.; Vandenberghe, I.; de Smet, L.; Frishman, D.; Nealson, K.H.; Cusanovich, M.A.; van Beeumen, J.J. Identification of 42 possible cytochrome *c* genes in the *Shewanella oneidensis* genome and characterization of six soluble cytochromes. *Omics* **2004**, *8*, 57–77. [CrossRef]
144. Meng, Q.; Sun, Y.; Gao, H. Cytochromes *c* constitute a layer of protection against nitric oxide but not nitrite. *Appl. Environ. Microbiol.* **2018**, *84*, e01255-18. [CrossRef]
145. Fredrickson, J.K.; Romine, M.F.; Beliaev, A.S.; Auchtung, J.M.; Driscoll, M.E.; Gardner, T.S.; Nealson, K.H.; Osterman, A.L.; Pinchuk, G.; Reed, J.L.; et al. Towards environmental systems biology of *Shewanella*. *Nat. Rev. Microbiol.* **2008**, *6*, 592–603. [CrossRef]
146. Kranz, R.G.; Richard-Fogal, C.; Taylor, J.S.; Frawley, E.R. Cytochrome *c* biogenesis: Mechanisms for covalent modifications and trafficking of heme and for heme-iron redox control. *Microbiol. Mol. Biol. Rev.* **2009**, *73*, 510–528. [CrossRef]
147. Meng, Q.; Yin, J.; Jin, M.; Gao, H. Distinct nitrite and nitric oxide physiologies in *Escherichia coli* and *Shewanella oneidensis*. *Appl. Environ. Microbiol.* **2018**, *84*, e00559-18. [CrossRef] [PubMed]
148. Fu, H.; Chen, H.; Wang, J.; Zhou, G.; Zhang, H.; Zhang, L.; Gao, H. Crp-dependent cytochrome *bd* oxidase confers nitrite resistance to *Shewanella oneidensis*. *Environ. Microbiol.* **2013**, *15*, 2198–2212. [CrossRef] [PubMed]
149. Zhang, H.; Fu, H.; Wang, J.; Sun, L.; Jiang, Y.; Zhang, L.; Gao, H. Impacts of nitrate and nitrite on physiology of *Shewanella oneidensis*. *PLoS ONE* **2013**, *8*, e62629. [CrossRef]
150. Zhou, G.; Yin, J.; Chen, H.; Hua, Y.; Sun, L.; Gao, H. Combined effect of loss of the caa_3 oxidase and Crp regulation drives *Shewanella* to thrive in redox-stratified environments. *ISME J.* **2013**, *7*, 1752–1763. [CrossRef]
151. Jin, M.; Fu, H.; Yin, J.; Yuan, J.; Gao, H. Molecular underpinnings of nitrite effect on Cyma-dependent respiration in *Shewanella oneidensis*. *Front. Microbiol.* **2016**, *7*, 1154. [CrossRef]
152. Yin, J.; Jin, M.; Zhang, H.; Ju, L.; Zhang, L.; Gao, H. Regulation of nitrite resistance of the cytochrome cbb_3 oxidase by cytochrome *c* ScyA in *Shewanella oneidensis*. *Microbiologyopen* **2015**, *4*, 84–99. [CrossRef]
153. Zemke, A.C.; Gladwin, M.T.; Bomberger, J.M. Sodium nitrite blocks the activity of aminoglycosides against *Pseudomonas aeruginosa* biofilms. *Antimicrob. Agents Chemother.* **2015**, *59*, 3329–3334. [CrossRef]
154. Zemke, A.C.; Kocak, B.R.; Bomberger, J.M. Sodium nitrite inhibits killing of *Pseudomonas aeruginosa* biofilms by ciprofloxacin. *Antimicrob. Agents Chemother.* **2017**, *61*, e00448-16. [CrossRef]
155. Zemke, A.C.; Shiva, S.; Burns, J.L.; Moskowitz, S.M.; Pilewski, J.M.; Gladwin, M.T.; Bomberger, J.M. Nitrite modulates bacterial antibiotic susceptibility and biofilm formation in association with airway epithelial cells. *Free. Radic. Biol. Med.* **2014**, *77*, 307–316. [CrossRef] [PubMed]
156. Zhang, Y.; Guo, K.; Meng, Q.; Gao, H. Nitrite modulates aminoglycoside tolerance by inhibiting cytochrome heme-copper oxidase in bacteria. *Commun. Biol.* **2020**, *3*, 269. [CrossRef] [PubMed]
157. Bueno, M.; Wang, J.; Mora, A.L.; Gladwin, M.T. Nitrite signaling in pulmonary hypertension: Mechanisms of bioactivation, signaling, and therapeutics. *Antioxid. Redox Signal.* **2013**, *18*, 1797–1809. [CrossRef] [PubMed]
158. Dunn, A.K.; Karr, E.A.; Wang, Y.; Batton, A.R.; Ruby, E.G.; Stabb, E.V. The alternative oxidase (AOX) gene in *Vibrio fischeri* is controlled by NsrR and upregulated in response to nitric oxide. *Mol. Microbiol.* **2010**, *77*, 44–55. [CrossRef]
159. Yoon, S.S.; Coakley, R.; Lau, G.W.; Lymar, S.V.; Gaston, B.; Karabulut, A.C.; Hennigan, R.F.; Hwang, S.H.; Buettner, G.; Schurr, M.J.; et al. Anaerobic killing of mucoid *Pseudomonas aeruginosa* by acidified nitrite derivatives under cystic fibrosis airway conditions. *J. Clin. Investig.* **2006**, *116*, 436–446. [CrossRef]
160. Feelisch, M.; Akaike, T.; Griffiths, K.; Ida, T.; Prysyazhna, O.; Goodwin, J.J.; Gollop, N.D.; Fernandez, B.O.; Minnion, M.; Cortese-Krott, M.M.; et al. Long-lasting blood pressure lowering effects of nitrite are NO-independent and mediated by hydrogen peroxide, persulfides, and oxidation of protein kinase G1α redox signalling. *Cardiovasc. Res.* **2019**, *116*, 51–62. [CrossRef]
161. Williams, D.E.; Nisbett, L.M.; Bacon, B.; Boon, E. Bacterial heme-based sensors of nitric oxide. *Antioxid. Redox Signal.* **2018**, *29*, 1872–1887. [CrossRef]
162. Anand, C.R.; Bhavya, B.; Jayakumar, K.; Harikrishnan, V.S.; Gopala, S. Inorganic nitrite alters mitochondrial dynamics without overt changes in cell death and mitochondrial respiration in cardiomyoblasts under hyperglycemia. *Toxicol. In Vitro* **2021**, *70*, 105048. [CrossRef]

163. Bailey, J.C.; Feelisch, M.; Horowitz, J.D.; Frenneaux, M.P.; Madhani, M. Pharmacology and therapeutic role of inorganic nitrite and nitrate in vasodilatation. *Pharmacol. Ther.* **2014**, *144*, 303–320. [CrossRef]
164. Rix, P.J.; Vick, A.; Attkins, N.J.; Barker, G.E.; Bott, A.W.; Alcorn, H., Jr.; Gladwin, M.T.; Shiva, S.; Bradley, S.; Hussaini, A.; et al. Pharmacokinetics, pharmacodynamics, safety, and tolerability of nebulized sodium nitrite (AIR001) following repeat-dose inhalation in healthy subjects. *Clin. Pharmacokinet.* **2015**, *54*, 261–272. [CrossRef]